3D River Discharge Modelling using UAV photogrammetry

Delft University of Technology

Niels Hoogendoorn

Master Thesis

3D River Discharge Modelling using UAV photogrammetry

by
N.J. Hoogendoorn

June 2023

A master thesis submitted to the Delft University of
Technology in fulfilment for the degree of
Master of Science
in Civil Engineering specialised in Water Management.

Assessment Committee:	Prof.dr.ir. N.C. van de Giesen
	Dr.ir. O.A.C. Hoes
	Dr.ir. D. Wüthrich
Supervisors:	Dr.ir. H.C. Winsemius
	M.A. S.V. Mather

TUDelft

Delft
University of
Technology

TEMBO Africa

Preface

Abstract

Water is essential for life on earth and is vital for numerous sectors of our society. Pressures arising from climate change, growing populations, and the shift towards clean energy accentuate the importance of effective water management. To make decisions about water resource allocation, hydraulic modeling studies have been undertaken on large African rivers. These studies employ global terrain models, utilize remotely sensed water surface elevation data, and often involve estimating river channel bathymetry. Typically, these models also require an estimation of the river channel bathymetry. However, observed bathymetry data is seldom available and crucial for the hydraulic model performance. It has resulted in a key challenge of modelling large rivers in this data-sparse context.

This research aims to model a medium to large sized river with wide floodplains in three dimensions by integrating discharge data and a highly accurate bathymetry. The primary objective is to quantify the friction coefficient and establish a reliable rating-curve for the river system. By utilizing these key components, the study seeks to provide a comprehensive understanding of the hydraulic behavior of the river, contributing to improved water flow predictions and management strategies. The bathymetry data is acquired through two different methods. The dry bathymetry is obtained using an UAV (DJI Phantom 4) and photogrammetry (WebODM). The wet bathymetry data is collected using both, sonar with the Deeper Chirp+ and spatial referencing with the RTK-GNSS from ArduSimple. These methods are cost-effective and require minimal manpower, making them practical options for acquiring accurate bathymetric information. The discharge data is acquired using the open-source software, OpenRiverCam. OpenRiverCam uses Large Scale Particle Image Velocimetry (LSPIV) to determine the surface velocities and combines the results with the bathymetry data to calculate discharges, providing an efficient solution for assessing river flow characteristics. LSPIV has the advantage that it is a non-intrusive method of measuring the flow velocity and does not require physical probes or instruments in the water. The bathymetry data and discharge data are integrated into the Delft3D FM Suite to assess the accuracy of the measurements and estimate the friction coefficient in both the river and the floodplain. This modeling approach enables a comprehensive analysis of the hydraulic characteristics of a medium to large sized river and supports the evaluation of flow resistance in the study area.

The data acquisition took place at three study sites close to the Bui Dam, in the Black Volta Region, Ghana. The Bui Dam is the second largest hydro-power dam in Ghana managed by the Bui Power Authority (BPA). The Bui Bridge and Bamboi Bridge study sites are positioned downstream of the Bui Dam, allowing for accurate quantification of the discharge and the bathymetry measurements. The third study site, Chache, is positioned upstream of the dam, where daily water level measurements are taken. BPA has observed that the rating curve at this location is outdated. Therefore, efforts are made to update the rating curve and quantify the friction coefficient at this site in both the river and the floodplain.

This research has made significant progress in developing a three-dimensional discharge model and rating curve for medium to large rivers using advanced data collection methods

Abstract

and integration techniques. The study successfully combined photogrammetry and sonar measurements to effectively determine the bathymetry of the river, overcoming challenges related to high water velocities and dense vegetation. The LSPIV technique and OpenRiver-Cam were utilized to integrate surface velocities and discharge measurements, leading to a more comprehensive understanding of river dynamics. However, limitations were encountered in assessing the accuracy of the model at the Bamboi Bridge site due to the LSPIV results. This highlights the importance of obtaining more comprehensive data and observations to enhance the model's accuracy. The comparison of rating curves at the Chache site resulted in positive results. Although, further verification during the wet period is required through velocity and discharge measurements to determine the accuracy. Overall, this research contributes to a better understanding of river behavior and provides valuable insights for water flow prediction in an efficient, cost-effective manner with minimal intensive manpower, ensuring a non-intrusive approach.

Contents

Contents

List of Figures

List of Figures

1. Introduction

1.1. Background

Water on earth is vital, our society depends on it in almost every sector. The changing climate, the rising population and the energy transition increase the pressure on water availability and the urgency of good water management and governance. Decision-making in the allocation of water resources is fundamental for sustainable development and human well-being [Connor, 2015], [Bertule et al., 2018]. To make these valuable, adequate decisions, monitoring networks are required. Unfortunately, in many parts of the world, monitoring networks are often inadequate and many are in decline due to fewer investments, social or political conflicts, and difficult and remote geographies [Dinku, 2019]. Also, most of the existing stations are unevenly distributed with more stations located in cities [Papa et al., 2022]. Due to this uneven distribution, it is often unclear what happens with the hydrological processes between the measuring stations. In order to gain a comprehensive understanding of the water system behaviour and make more efficient decisions regarding water allocation, it is crucial to conduct measurements in these remote areas as well. Remote sensing offers a solution, especially in data-scarce areas. It has already been shown to be powerful for monitoring and modelling large water bodies [Schumann et al., 2008]. Particularly, for flood analysis, where monitoring infrastructures are vulnerable, costly and possibly exceed their measuring capabilities, remote sensing provides a robust and viable alternative. Currently, water depths are mainly measured using remote sensing, with vertical accuracies up to 3 centimeters with the new SWOT and SKIM satellite missions [Morrow et al., 2019], [Ardhuin et al., 2019]. Additionally, with very high spatial resolutions (50 cm/pix), it is also possible to determine the stream flow rates of the largest rivers from space using Large Scale Particle Image Velocimetry (LSPIV)[Everard et al., 2023]. LSPIV uses the motion of visible features on the surface water tracked through time [Fujita et al., 2019]. However, bathymetry, which is a very important factor in the accuracy of hydrological models and the estimation of discharge from surface velocity, is still hard to determine from space. The river color and turbidity, together with the vegetation and the need for high resolutions make it difficult for satellite signals to distinguish river bottoms. To effectively obtain quantitative spatially distributed data of the bathymetry over large areas, sonar and photogrammetry can be used.

1.2. Problem Statement

Several hydraulic modelling studies have been conducted on large rivers in Africa [Kittel et al., 2018], [Stisen et al., 2008], among others. They have in common that they utilize global terrain models to map floodplains and main river channels and rely on (remotely sensed) observations of water surface elevations with sometimes some other parameters. Typically, these models also require an estimation of the river channel bathymetry. This is often done by treating it as a parameter to be calibrated alongside the friction coefficient.

However, observed bathymetry data is seldom available and crucial for the hydraulic model performance. It has resulted in a key challenge of modelling large rivers in this data-sparse context [Jung et al., 2010], [Papa et al., 2022].

1.3. Research Question

This research aims to model a medium to large sized river with wide floodplains in three dimensions by integrating discharge data and highly accurate bathymetric data. The primary objective is to quantify the friction coefficient and establish a reliable rating-curve for the river system. By utilizing these key components, the study seeks to provide a comprehensive understanding of the hydraulic behaviour of the river, contributing to improved water flow predictions and management strategies. The bathymetry data is acquired through sonar and photogrammetry. These methods are cost-effective and require minimal manpower, making them practical options for acquiring accurate bathymetric information. The discharge data is acquired using the open-source software, OpenRiverCam. OpenRiverCam uses Large Scale Particle Image Velocimetry (LSPIV) to determine the surface velocities and combines the results with the bathymetry data to calculate discharges, providing an efficient and non-intrusive solution for assessing river flow. The bathymetric data and discharge data are integrated into a Delft3D FM Suite model to assess the accuracy of the measurements and estimate the friction coefficient in both the river and the floodplain.

"How to create a three-dimensional discharge model and rating curve of a middle to large river using a high precision bathymetry based on photogrammetry, sonar, RTK-GNSS and large scale image velocimetry data?"

The main research question will be answered based on the answers from the following sub-questions:
How can the photogrammetry and the sonar measurements be combined to obtain the bathymetry of the river?
What are the methods and approaches for integrating surface velocities into a discharge model?
To what extent can the Manning's friction coefficient of the river channel and floodplain for medium to large rivers be accurately quantified?

Answers to the research questions will be obtained during fieldwork at the Black Volta River in Ghana, Africa, close to the Bui dam. The data is collected over 2 months and processed after.

1.4. Outline of the report

Chapter 2 provides an overview of the research area and specific study sites, followed by a detailed discussion of the various data collection methods in Section 2.3. The subsequent sections delve into the data processing, Section 2.4, and modeling techniques, Section 2.5). In Chapter 3, a comprehensive analysis and interpretation of the obtained results is presented, leading to the conclusive findings and the answer to the main research question in Chapter 4. Lastly, Chapter 5 provides recommendations for future studies.

2. Materials and methods

This chapter begins by providing a description of the study area where the fieldwork is conducted. It then outlines the methods utilized to address the research questions and sub-questions, along with the necessary materials for implementing these methods.

2.1. Research Area

The location of the assembled data is in Ghana, more accurately at the Bui dam at the border of Brong-Ahafo and the Northern region. The river is transboundary and is called the Black Volta River. The river runs from Mali (11%) through Burkina Faso (59%) and Côte d'Ivoire (8%) and ends in Ghana (22%). The Black Volta tributary is the biggest sub-catchment of the Volta Catchment and has a mean annual flow of around 7.8 km^3/year. The mean annual flow at the Bui dam is around 7.1 km^3/year according to Shaibu et al. [2012]. The construction of the Bui Dam was finished in 2013 and is since managed by the Bui Power Authority (BPA). The reservoir has a total volume of 12.57 km^3, with approximately 48 percent of it being active storage BPA [2012]. So, the yearly mean inflow is 17 percent higher than the total volume of the reservoir. BPA has measured inflow data at the Bui dam which shows that the annual average, maximum, minimum and coefficient of variation of flow for all the months of the period 1954–2010 are respectively 227.6 m^3/s, 612.2 m^3/s, 70.7 m^3/s and 40% [Akpoti et al., 2016]. The Bui dam has a capacity of 404 MW electricity production making it the second largest hydro-power dam of Ghana [BPA, 2012].

Figure 2.1.: The Bui Dam

The fieldwork is conducted from February to early May (2023) which coincides with the end of the dry season (Figure 2.2).

(a) Mean day and night temperatures (°C)   (b) Mean precipitation (mm/day)
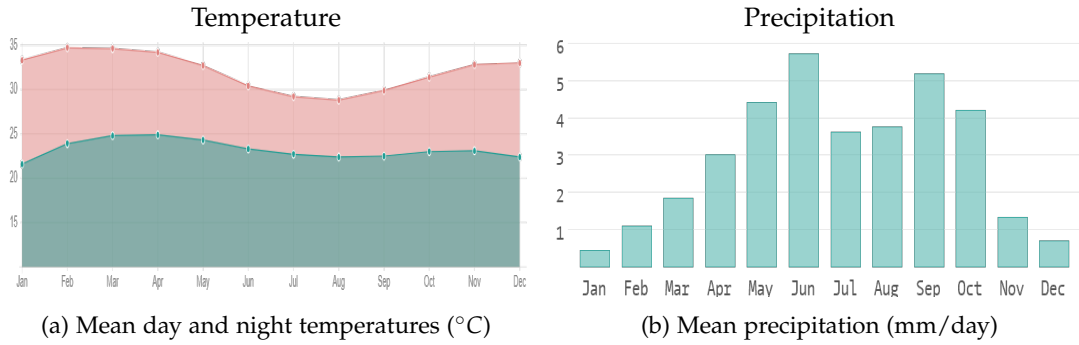
Figure 2.2.: Monthly mean temperature and precipitation in Ghana [Worlddatainfo, 2023].

The Black Volta catchment has a largely tropical wet or savannah climate in the south and a smaller hot semi-arid or steppe climate in the north [Beck et al., 2018]. Dominant class types are grasslands and agricultural land in the north and forest evergreen and forest deciduous in the south (Figure 2.3).
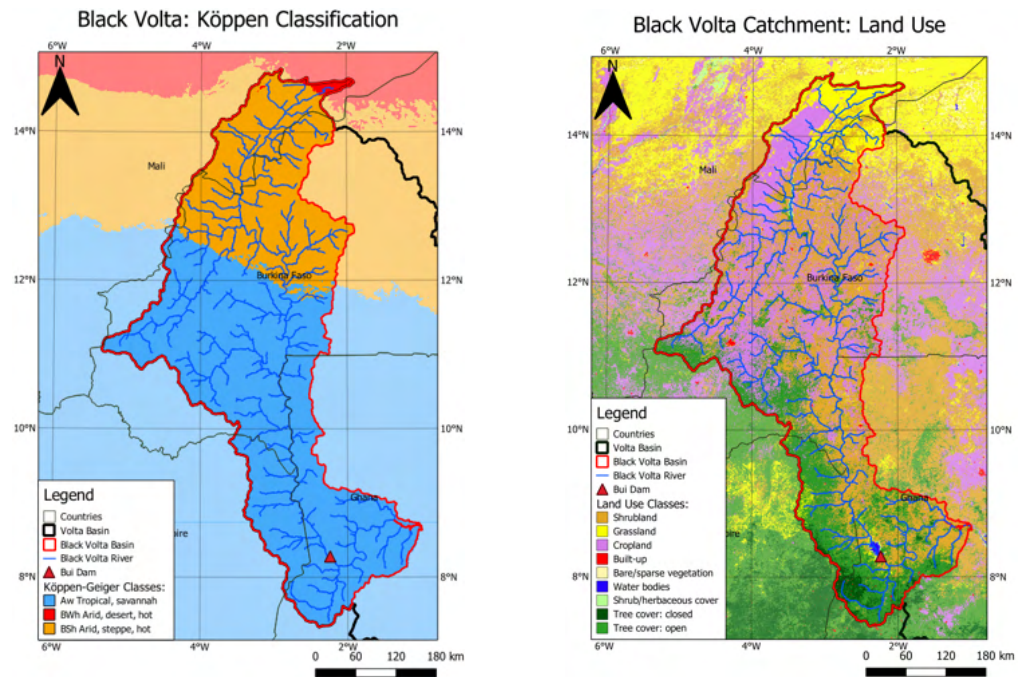
Figure 2.3.: Köppen-Geiger Climate and Land Use classification in the Black Volta Catchment (based on data from: Beck et al. [2018]).

2.2. Study sites

Fieldwork is conducted at three locations: Chache, the Bui Bridge and the Bamboi Bridge. See Figure 2.4 for the location and Figure 2.6 and Appendix D for areal photos of the sites.
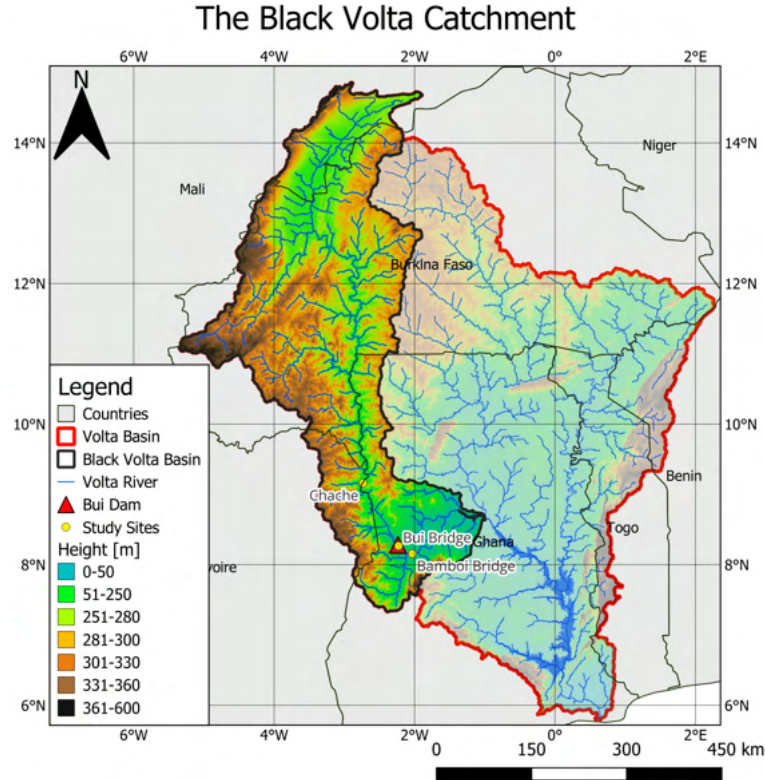
Figure 2.4.: Black Volta Basin (based on data from: Lehner and Grill [2013]).

2.2.1. Chache

Chache, located approximately 130 kilometers upstream of the Bui Dam on the border with Côte d'Ivoire, currently has limited accessibility with only a small ferry crossing the Black Volta River. In this remote location, BPA relies on manual water depth measurements using a staff gauge due to poorly maintained equipment and the lack of a stable internet connection, making automated data transfer challenging. However, this is set to change as a new bridge is being constructed, facilitated by Côte d'Ivoire, to improve transportation between the two countries. Chache holds significant importance for BPA, particularly in relation to inflow casting. The travel time for water between Chache and the Bui reservoir is approximately three days, making it a crucial location for accurate inflow calculations. Together with Lawra, located upstream with a travel time of five days, Chache forms the foundation for decision-making in anticipating electricity production during expected peak and low discharge periods. The forthcoming bridge construction will not only improve transportation but also provides the opportunity to contribute to the efficiency and reliability of data collection at this site.

At present, the inflows of the reservoir are estimated using a rating-curve established by BPA during the dam's feasibility study prior to 2013. This rating-curve equation

$$Q = 21.5 * (H - 0.55)^{2.4} \tag{2.1}$$

relates discharge (Q) to water height (H). The precise process by which this rating curve was derived is no longer entirely clear, but it was said to involve conducting various measurements using an Acoustic Doppler Current Profiler (ADCP) and extrapolation of the obtained results (BPA). While this rating-curve is still in use, BPA is interested in obtaining an updated version. In a recent study by Kasteel [2023], a new rating-curve was developed based on a conservative approach, incorporating the reservoir water balance, daily water height measurements at the Bui Dam, evaporation rates, local precipitation, and the reservoir volume curve. The equation of the new rating-curve is given as

$$Q = 20 * (H - 0.32)^{2.27} \tag{2.2}$$

Both equations are displayed in Figure 2.5. BPA is particularly interested in exploring not only data-driven rating-curve approaches but also physically-based methods, hence the reason for choosing this study site. The results of Delft3D FM Suite, Section 3.3, based on photogrammetry and sonar data of Chache are compared with these rating-curves and aims to assess the accuracy between the methodologies.
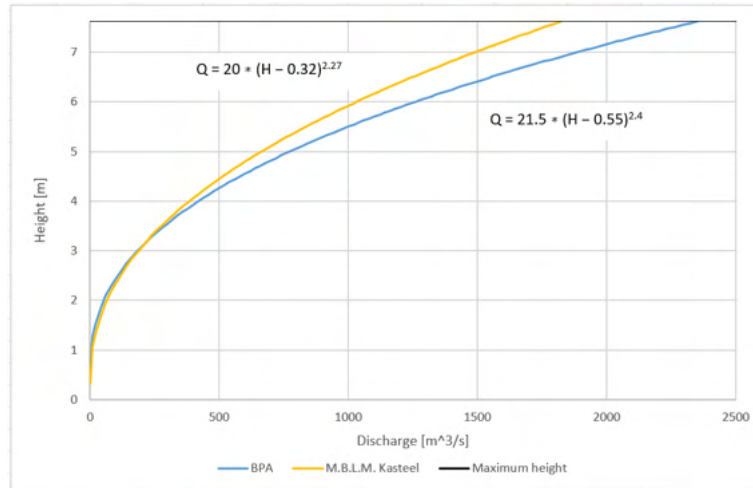
Figure 2.5.: Rating-Curves Chache, from: BPA [2012]), Kasteel [2023]

During the fieldwork conducted during the dry season, the river is approximately 120 meters wide and has a maximum depth of around 3.2 meters. However, according to BPA, the river expands significantly during the wet season, reaching widths of up to one kilometer and water depths of 7.62 meters. This is measured using 8 staff-gauges which are levelled using a total station leveller and remeasured every 2 years during maintenance. Unfortunately, due to time restrictions, this research does not include fieldwork during the wet season. However, it is possible to determine the bathymetry of the floodplain with photogrammetry while the floodplain is still dry. During measurements, it is essential to consider the variation in discharge. The flow velocities differ significantly, with negligible velocities during the dry season and high velocities during the wet season. The depth profile of this section of the river is very homogeneous, with dense vegetation along the sides of the river and slightly less in the floodplains.

2.2.2. The Bui Bridge

The second location is at the Bui Bridge, approximately 1.7 kilometers downstream of the Bui Dam. Due to the known electricity production and consequently the outflow rate, this location serves as a suitable site for assessing the accuracies of the methods employed in this research. Also, automated daily depth measurements are conducted by BPA at this location. The river has a width of around 100 meters and the fluctuations in depth are little, due to the regulated outflow from the dam. Only during spillages of the dam, this can change drastically. The Bui bridge is relatively close to the dam and the bed of the river is therefore still rocky and heterogeneous. This causes irregular and high (surface) flow velocities that must be taken into account during measurements. This location has also a lot of vegetation in the riverbanks.

2.2.3. The Bamboi Bridge

The Bamboi Bridge is the third study site, situated approximately 32.2 kilometers downstream of the Bui Dam. This location features a meandering river with a sandy and spatially homogeneous riverbed, similar to the characteristics observed at Chache (subsection 2.2.1). This similarity makes Bamboi Bridge an ideal location for testing the methods employed in this research, particularly in relation to bathymetry measurements. A disadvantage of this location is the distance between the Bamboi Bridge and the Bui Dam making it challenging to determine the travel time of water and, consequently, compare discharge values. Additionally, there is a river tributary between these two locations, which can result in different flow rates. It is important to consider these factors when analyzing the data collected at the Bamboi Bridge site. BPA measures the river depth at the Bamboi Bridge only during spillage of the Bui dam using staff gauges.

(a)

(b)

(c)
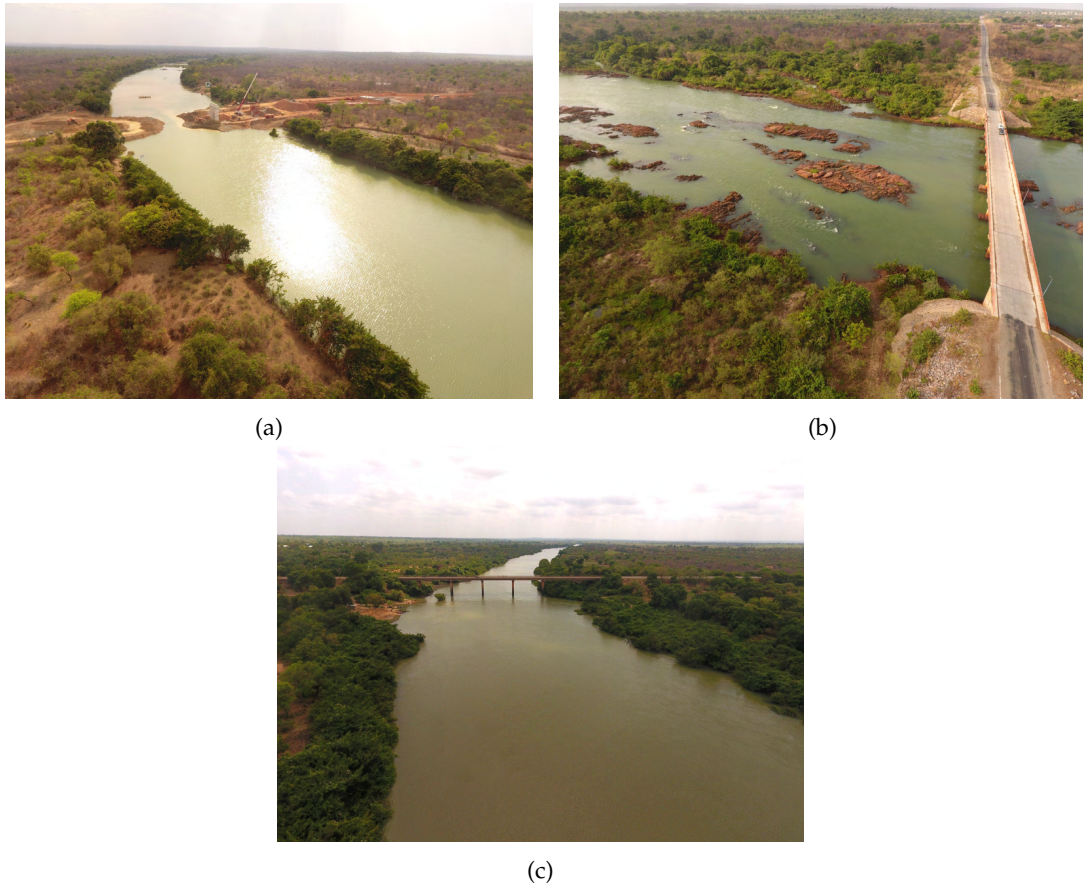
Figure 2.6.: Areal Photos: (**a**) Chache, with the new bridge still in construction, 16-03-2023. (**b**) Bamboi Bridge, 03-03-2023. (**c**) Bui Bridge, 21-03-2023.

2.3. Data Collection

To address the main research question, "How to create a three-dimensional discharge model and rating curve of a middle to large river using high-precision bathymetry based on photogrammetry, sonar, RTK-GNSS, and large-scale image velocimetry data?", various materials and methods were employed.
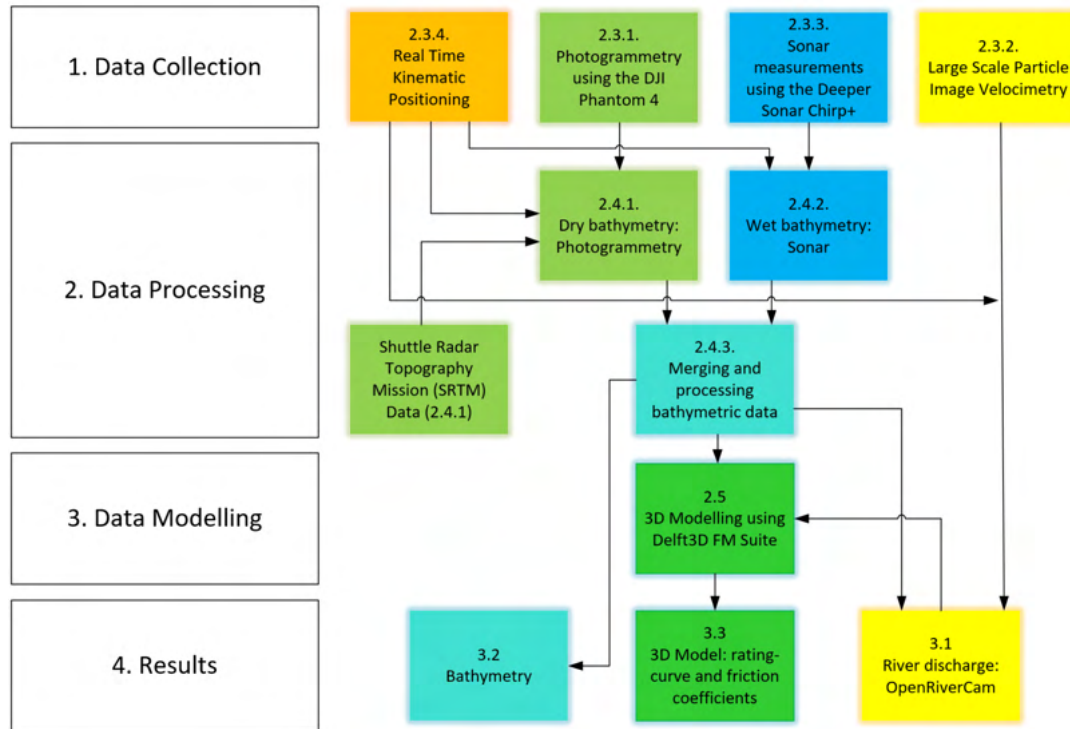
Figure 2.7.: Overview

Traditionally, acquiring river discharge data and establishing accurate rating curves involves on-site measurements across different flow conditions and inter- and extrapolation of the results. However, the combination of photogrammetry and LSPIV through the use of a UAV provides a more streamlined approach to evaluating both the physical and hydraulic attributes of a river. This allows for a quicker and more timely development of accurate rating curves [Westerberg et al., 2023]. Subsections 2.3.1 and 2.3.2 provide detailed explanations of these methods. It is important to note that this methodology is applicable primarily in clear rivers, as photogrammetry cannot effectively measure bathymetry in turbid waters. In such cases, sonar measurements (as elaborated in Subsection 2.3.3) are utilized to obtain bathymetric data. This data is then merged with the photogrammetry data through RTK-GNSS (outlined in Subsection 2.3.4). The merging process of sonar and photogrammetry is more extensively explained in Subsection 3.2.3 to address the sub-research question: "How can the photogrammetry and the sonar measurements be combined to obtain the bathymetry of the river?" To construct a 3D river discharge model in Delft3D FM Suite, the comprehensive bathymetry is combined with the acquired river discharge and surface velocity data, as described in Section 2.5. This process addresses the research question: "What are the methods and approaches for integrating surface velocities into a discharge model?" Furthermore,

the extent to which the Manning's friction coefficient of the river channel and floodplain for medium to large rivers can be accurately quantified is also determined within this section, aligning with the question: "To what extent can the Manning's friction coefficient of the river channel and floodplain for medium to large rivers be accurately quantified?" Figure 2.7 provides an overview of the relationships between the different data collection, processing, modelling, and resulting outcomes.

2.3.1. Photogrammetry using the DJI Phantom 4 (UAV)

The riverbed and cross-section of the river are the physical characteristics for establishing a rating-curve and a 3D model. Determining this bathymetry by hand can be very time-consuming and highly location specific, due to disturbances caused by large boulders or holes in the river. Fortunately, LIDAR and photogrammetry can provide detailed and precise measurements of the bathymetry on larger areas. These technologies reduce reliance on manual measurements and offer greater flexibility in conducting measurements at different locations. In this research, photogrammetry is used with the affordable DJI Phantom 4 UAV (DJI-P4). The imagery is collected while flying in a predefined grid with the application Pix4Dcapture and is later post-processed (subsection 2.4.1). The accuracy of the photogrammetry relies greatly on the flight grid which is dependent on the location and vegetation. The land use at the study sites is classified as shrubland and open tree-covered, Figure: 2.3), with more vegetation along the sides of the river. To maximize the acquisition of bathymetric information, it is preferable to conduct oblique flights, allowing for the capture of imagery that reveals submerged features beneath vegetation or obstacles such as trees (Peppa et al. [2019]). In UAV photogrammetry surveys, the camera can be pre-calibrated or can be calibrated "on-the-job" using structure-from-motion and a self-calibrating bundle adjustment. The magnitude of the systematic error is influenced by camera specifications (sensor format, lens focal length, etc.), camera calibration accuracy, camera network geometry, the distribution and accuracy of ground control and the precision with which targets can be measured and matched. In general, when enough Ground Control Points (GCP) are established (at least 5 depending on the surveying size), on-the-job calibration is more accurate than pre-calibration, but it has its limitations in determining river slopes due to the 'doming' and 'bowling' effect Griffiths and Burningham [2019]. Doming and bowling in UAV photogrammetry refer to distortion in images caused by sloping or curved surfaces, leading to inaccuracies in 3D models and point cloud data.

2.3.2. Large Scale Particle Image Velocimetry

Large Scale Particle Image Velocimetry (LSPIV) is utilized to determine the discharge and surface velocities in the Black Volta River. LSPIV analyses images of the river taken from an elevated position (UAV or Video Camera) with very short time steps and compares the particle movements such as eddies and debris on the surface of the water to determine the surface velocities. LSPIV has the advantage that it is a non-intrusive method of measuring the flow velocity, does not require physical probes or instruments in the water and can cover large areas with relatively high spatial resolution. It even has the flexibility to be employed in flood situations, utilizing videos captured with mobile phones. The requirements of the videos are: a video duration between 5 to 30 seconds depending on the river size, surface velocities and amount of particles that can be traced; six GCPs (exact locations) for the orthographic projection of the images; a known water level during the videos; and one or

more cross-sections of the river. The open-source software OpenRiverCam is used for this. It is able to convert the (UAV) camera videos into surface/river flow velocities and facilitate the integration of these flow velocities with the bathymetric data of 2.4.1 for determining discharge. Additionally, if enough videos (a minimum of 5) with different water heights are made, the program is also able to establish a rating curve automatically.

2.3.3. Sonar measurements using the Deeper Chirp+

The wet bathymetry of the Black Volta River cannot effectively be captured using photogrammetry because the water is too turbid. To overcome this limitation sonar is used. The price range of sonar is very wide so for this research, a practical and cost-effective solution is used, namely the Deeper Sonar Chirp+.

<div align="center">(a)   (b)</div>

Figure 2.8.: (**a**) The attachment of the cost-effective Deeper Sonar Chirp+ and the RTK-GNSS on the floaters. (**b**) Measuring the wet bathymetry of the Black-Volta River using a local fisherman his canoe.

The Deeper Sonar Chirp+ is commonly used by anglers to see where the good spots are before casting their rod. You can attach it to your boat or your fishing rod and it uses sound/sonic navigation and ranging (Sonar) to know where fish are. It stores, among others, the location where it has been, the amount of fish at that particular location and the depth in the application Fish Deeper. While it may have limitations in accuracy and resolution compared to more advanced alternatives, it offers an accessible means of acquiring essential depth information for this research purpose. The Deeper Sonar Chirp+ connects with your phone using a Wi-Fi connection and has a range of 100 meters. It can measure depth with three different angles ($47°$, $20°$, $7°$), with the smallest angle being the most location specific. When the measurements are not significantly affected by water turbidity it can measure depth with an accuracy of 2.1% for depths up to 35 meter[Bandini et al., 2018]. The minimum depth is 15 centimeters and the maximum depth is 100 meters. The Deeper Sonar Chirp+ has two useful location options, the Onshore- and Boat mode. The Onshore mode uses the GPS-Receiver within the Deeper Sonar Chirp+. The Boat mode connects immediately to the

GPS of the phone. However, both modes have often an accuracy in meters, which is not sufficient for achieving accurate river bathymetry. Therefore, the RTK positioning described in subsection 2.3.4, which has a centimeter accuracy, is used instead. The simpleRTK2B rover is connected with USB OTG to the phone and the application SW Maps - GIS & Data Collector is used to change the GPS of the phone to the more accurate RTK-GNSS positioning (location mocking). Figure 2.8a shows an overview of the setup. The setup is utilized in two distinct ways: when the velocities in the water were too high a rope was suspended from a bridge and when the conditions were safe the setup was placed next to a canoe and the measurements were done from there.

2.3.4. Real Time Kinematic Positioning

Both photogrammetry and sonar measurements rely on relative positioning, meaning they provide information based on the relationships between different points. To accurately combine these measurements, it is required to establish a common absolute positioning reference. In this study, a Real-Time Kinematic Global Navigation Satellite System (RTK-GNSS) is employed to fulfil this requirement. As the name suggests, RTK can provide real-time data to achieve reliable positioning accuracy. It utilizes phase differences in the GNSS signals to correct its position. The RTK-GNSS is employed for both the determination of the GCPs during photogrammetry and the accurate positioning during the Sonar measurements. In this research, a base-rover approach is used which has a minimal accuracy of 2 centimeters for distances smaller than 20 kilometers [Feng et al., 2008].

(a)
(b)

Figure 2.9.: (**a**) The simpleRTK2B - Starter Kit LR, from: ArduSimple [2023]) (**b**) Setup of the simpleRTK2B base together with the BPA staff.

Figure 2.9a shows the simpleRTK2B - Starter Kit LR module. It contains two simpleRTK2B boards. One of the boards is preconfigured as the base and the other as the rover. The boards are communicating with Long Range (LoRa) modulus. LoRa is defined as a low-power wide area network protocol. The two antennas are added for better reception. The maximum distance is around 10 kilometers depending on the signal noise[Feng et al., 2008]. The two simpleRTK2B boards receive GNSS Dual Band with the U-blox ANN-MB-00 Antennas which contains the RTK positioning data. The base requires several hours for configuration

to increase in absolute accuracy. As earlier mentioned, there is a lot of vegetation on the river banks at the study sites. Measuring the GCPs is rather difficult because the line of sight can be obstructed due to this vegetation.

2.4. Data Processing

The dry- and wet bathymetry have to be merged, but they are first individually post-processed. The discharge is determined using LSPIV and the cross-sections obtained from the merged bathymetry.

2.4.1. Dry bathymetry: Photogrammetry

The obtained two-dimensional images from the study sites are converted into a three-dimensional point cloud using Structure from Motion (SfM) derived photogrammetry software called WEB Open Drone Map (WebODM). WebODM generates geo-referenced maps, point clouds and textured 3D models [OpenDroneMap, 2023]. Figure 2.10 is an example of the point cloud from the Bamboi Bridge site. Two steps have been taken to get the most accurate representation of the dry bathymetry. The steps were mainly executed using the Point Data Abstraction Library (PDAL).
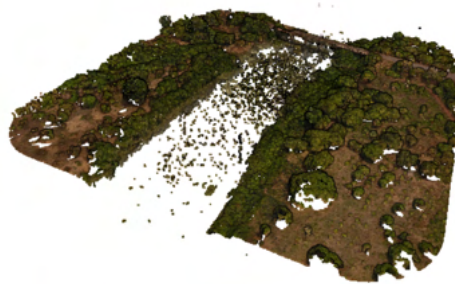
Figure 2.10.: Example of a 3D point cloud of the Bamboi Bridge site (21/3/2023), made with: OpenDroneMap [2023])

1. Filtering
WebODM classifies the point-clouds in categories such as ground, low-vegetation, buildings, etc. Only the 'Ground' classification is required for the dry bathymetry. There were still some outliers, mainly in the water, probably due to the reflection of the water. These are filtered by limiting the maximum and minimum height (z) and excluding all points in a self-made wet bathymetry polygon.

2. Interpolation
The UAV photogrammetry survey is conducted using a double grid approach, with an oblique angle of 20 degrees, as well as with a circular grid flown at a height of 45 meters 2.3.1. However, certain data are still missing due to blockage caused by vegetation. Additionally, there are some gaps in the data due to the filtering processes. To address this, linear interpolation is employed to fill the gaps and generate a more comprehensive and continuous data set for further analysis.

Typically, the interpolated grid is sufficient for merging with the wet-bathymetry data. However, in this case, it was observed that the interpolated grid did not accurately represent the actual bathymetry due to the presence of vegetation, which caused noise resulting in elevated measurements along the sides of the river. This discrepancy was likely a result of inaccurate vegetation classification. To address this issue, two alternative approaches were tested. In the first approach, the area affected by vegetation-induced noise is masked and subsequently interpolated. The second approach utilizes the Grass GIS tool r.geomorphon, which provides a more general method for addressing the issue. Figure 2.11 illustrates the presence of hills close to the side of the river in cross-sections 2 and 3, while cross-sections 1 and 4 illustrate a smooth transition to the water level.

(a) (b)
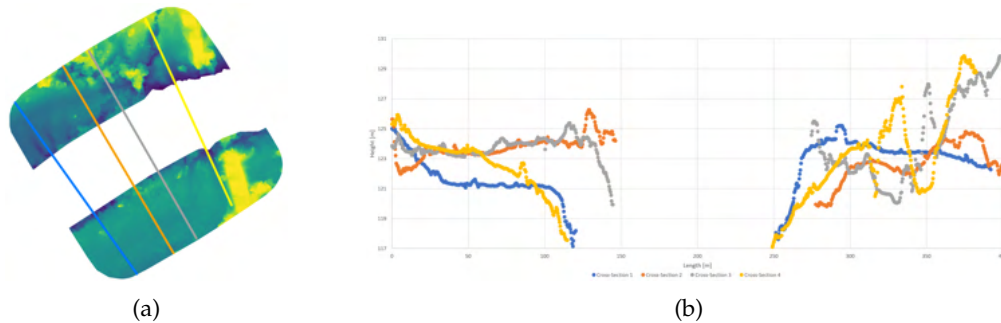
Figure 2.11.: (**a**) Bamboi Bridge DTM with cross-section. (**b**) The cross-sections (Colors match with a). Cross-sections 2 and 3 show small hills or stop abruptly instead of going smoothly to the water level, caused by vegetation being interpreted by WebODM as the ground surface.

2.4.2. Wet bathymetry: Sonar

The data collection process described in subsection 2.3.3 yields a CSV-file containing the xyz coordinates. In this file, the height coordinates (z) are relative to the water level, which is required to be constant throughout the execution. The relative height coordinates are converted to absolute values using the water height measured with the RTK-GNSS. The point data on its own is very location dependent, but the results demonstrate that the bathymetry is relatively homogeneous at the Chache and Bamboi Bridge sites, allowing for reliable interpolation between values in order to obtain a Digital Elevation Map (DEM). In contrast, the Bui-Bridge site presents a rocky and heterogeneous riverbed making it untrustworthy to do any assumptions about the riverbed characteristics, especially with the limited bathymetric data. The interpolation will be executed in Python using mainly Pandas, GeoPandas and the Scipy library. The collected point data for the Chache and Bamboi Bridge sites are obtained in a grid sailed by canoe. As a consequence, the curvature of the river cross-section makes direct interpolation between these points an inaccurate representation of reality, because the grid lines orthogonal to the river flow hold more information on the depth data for locations parallel to those points than the grid lines already directed parallel to the river flow, which is shown in figure 2.12. This inconsistency highlights the importance of considering the spatial distribution of data when interpreting and interpolating bathymetric information. If the same number of points were collected for the grid lines parallel to the direction of the flow and perpendicular to the direction of the flow, this method can be avoided, but this is

practically (sailing in a canoe) almost impossible.
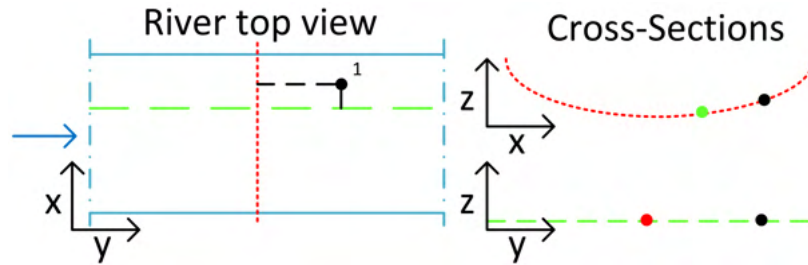
Figure 2.12.: A simplification of a homogeneous riverbed with two bathymetric grid lines, showing that although the bathymetric grid line parallel to the river flow (green) is closer to point 1, the grid line perpendicular to the river flow (red) contains more accurate depth information about point 1, because the perpendicular grid line contains the curvature of the cross-section. (For clarity, the river slope is not depicted in the drawing since it is negligible compared to the height difference in the cross-section. The coloured points indicate the intersections of the cross-sections.)

To solve this interpolation problem, a higher 'importance' to the orthogonal grid lines is desired when interpolating. To achieve this, the following steps have been applied: (also shown in 3.6 and Appendix A). First, the grid is rotated, so that the river is parallel to the x-axis. Secondly, the grid is scaled in the y direction resulting in larger distances between the grid lines that are directed parallel to the river flow. Thirdly, the grid is interpolated to obtain the DEM and due to the larger distances the influence of the orthogonal grid lines is much higher than the influence of the parallel grid lines. Finally, the DEM is re-scaled and re-rotated, resulting in a DEM that accurately follows the curvature of the river. Multiple interpolation approaches were evaluated based on the most realistic fit, including inverse distance weighted (IDW), cubic, and linear interpolation. The linear interpolation method was selected as it resulted in bathymetry data that did not exhibit any unusual or unrealistic shapes.

The DTM of the dry-bathymetry acquired through UAV surveying is larger in scale compared to the DTM of the wet-bathymetry. In order to estimate representative values for the wet-bathymetry in areas where data is missing, a mean cross-section is determined which shifts with the meandering curve of the river. The slope of the river is added over the direction, parallel to the flow direction (Figure: 3.6f). This approach is feasible due to the consistency and homogeneity of the river at the study sites. The slope was not measured directly during the fieldwork, because the overhanging vegetation made it impossible to measure the side of the river while maintaining an unobstructed line of sight between the RTK-GNSS rover and base. The slope is therefore determined in two different methods and compared afterwards. The first method involves the usage of the dry-bathymetry DTM from subsection 2.4.1. In this DTM, areas are selected at the water-land boundary and converted into a line-string containing the depth-distance information. From this line-string is the slope determined. Due to the doming and bowling effect explained in subsection 2.3.1, this method is not ideal. The second method utilized several Shuttle Radar Topography Mission (SRTM) Digital Elevation Maps. Similarly, a line-string was created along the river for several kilometers, and the depth information was used to calculate the slope. It is important to note that the minimum vertical accuracy of the SRTM DEM is 16 meters in absolute error with a 90% confidence (Root Mean Square Error (RMSE) of 9.73 m) worldwide [Mukul

et al., 2017]. Consequently, this method can only be used to determine slopes on a large scale and is not locally applicable. However, this specific section of the Black Volta River has a relatively gentle and constant slope over a long distance, making it still suitable for this method's application.

2.4.3. Merging and processing bathymetric data

The wet- and dry bathymetry are post-processed as explained in previous subsections and are now merged in two steps, answering the sub-research question: "How can the photogrammetry and the sonar measurements be combined to obtain the bathymetry of the river?". First, the GRASS GIS tool 'r.patch.smooth' is utilized to merge and smooth the overlapping bathymetric sections. The smoothing distance is determined based on achieving the most accurate representation of reality. While this process is somewhat subjective, the resulting changes have minimal impact on the bathymetry result. Second, the gaps in the bathymetry are interpolated linearly using the QGIS fill-gaps tool, the overall obtained resolution is 0.01 square meters. The bathymetric data covers a 400x400 meter area. However, it should be noted that at the Chache site, the floodplains are wider. The UAV Photogrammetry could not capture this entire floodplain due to its limited battery life. To address this, the bathymetric data is extended by integrating SRTM Digital Elevation Maps, which have a tile width of 30x30 meters. While not ideal, this approach matched the existing data reasonably. However, the absolute accuracy of bathymetry outside the 400x400 meter area is considerably lower as a result. This will certainly be taken into account while analyzing the data. In order to use the merged bathymetric data in the Delft3D FM Suite (section 2.5), more steps have to be taken. To ensure that the river remains in a steady state throughout the full bathymetric model, an extended length is employed. This extension of the river length ensures that the downstream boundary conditions have a negligible influence on the results, with a difference of less than one centimeter. The extensions are based on the full cross-sections both up and downstream. To accomplish this, the complete bathymetry data is once again imported into Python. Following the same rotation procedure described in subsection 2.4.2, a cross-section is computed and subsequently simplified. The cross-sections are then incrementally added at 1-meter intervals, resulting in the creation of a new point cloud. This point cloud is further converted into an XYZ-file format, allowing it to be imported into the Delft3D FM Suite.

2.5. 3D Modelling using Delft3D FM Suite

This concluding section of this chapter outlines the methodology employed for constructing the 3D discharge model, providing a comprehensive understanding of the flow dynamics within the river system. In doing so, all the collected and processed data is utilized to provide an answer to the mean research question: "How to create a three-dimensional discharge model and rating curve of a middle to large river using a high precision bathymetry based on photogrammetry, sonar, RTK-GNSS and large scale image velocimetry data?" The three dimensional data modelling is conducted using the Delft3D D-Flow Flexible Mesh Suite (Delft3D FM). Delft3D FM is an Open Source Software and facilitates hydrodynamic (Delft3D-FLOW module), morphodynamic (Delft3D-MOR module), waves (Delft3D-WAVE module), water quality (Delft3D-WAQ module including the DELWAQ kernel) and particle (Delft3D-PART module) modelling [Deltares, 2013]. For this research, only the flow module

will be used. The basis of this model is the non-linear shallow water equation, derived from the Navier-Stokes equations, taking into account the conservation of mass and momentum. Several assumptions are made for modelling river flow, such as the neglect of water flux through the river bed, zero exchange of water with the free surface, and simplified treatments of vertical velocities from the continuity equation and density effects in the pressure term. The Delft3D software is able to use structured or unstructured grids, with options for sigma and Z layering methods in three-dimensional models. Boundary conditions, including inflow and outflow, are necessary for simulating desired hydraulic processes. The upper boundary condition is discharge in the used model and the lower boundary condition is river height. The lower boundary condition is set at a greater distance to minimize its influence on the behaviour and dynamics within the main area of interest. If the lower boundary condition were set too close to the area of interest, it could introduce unwanted effects and distortions in the results. The river height is determined through an iterative process, requiring a constant water depth with a tolerance of less than a centimeter difference. An initial condition for the water level is set as well so that the steady state in the modelled river is reached faster, this reduces the required modelling time. Physical parameter values, such as the friction coefficients are calibrated to fit the model test data. There are three options in the Delft3D FM Suite to calculate the flow velocity in an open channel, namely with Manning, Chézy and White-Colebrook. They are all three based on a friction coefficient and for this research Manning is chosen. It relates the flow velocity (V) to the hydraulic radius (R), the hydraulic slope (S) and the Manning's roughness coefficient (n). While Delft3D FM solves the nonlinear equation for shallow water flow including friction, the Manning's equation is presented here in steady-state and one-dimensional form for comprehensibility:

$$V = \frac{1}{n} * R^{2/3} * S^{1/2} \tag{2.3}$$

Where: V is the flow velocity [m/s], n is the Manning's roughness coefficient [$s/m^{1/3}$], R is the hydraulic radius (defined as the cross-sectional area of flow divided by the wetted perimeter)[m], S is the hydraulic slope (defined as the change in water surface elevation per unit length of the channel)[-].

The Manning's friction coefficient can be distributed spatially, with separate components for the floodplain and the river channel, where limited data is available for the latter. According to Chow [1959], Manning's friction coefficient for channels can range from 0.03 (clean) to 0.1 (very weedy/rocky reaches), while for floodplains, it can vary from 0.03 (pasture short grass) to 0.150 (heavy stands of timber and a few fallen trees). Two 3D models are made, one representing Chache and the other representing the Bamboi Bridge.

At the Bamboi Bridge site, the objective is to compare and assess the precision of Open-RiverCam measurements against the discharge and surface velocities obtained from the Bui Dam, utilized in the three-dimensional model. This is facilitated by the known scaling factor used by OpenRiverCam, where the depth-average velocity equals the surface velocity multiplied by 0.85. This approach addresses the sub-research question "What are the methods and approaches for integrating surface velocities into a discharge model?" In this context, assumptions must be made regarding the friction coefficient in both the river channel and floodplain, these are made based on research by Arcement Jr et al. [1984]. If the results match well, the depth-average velocity outcomes from Delft3D FM and OpenRiverCam can

be equated to determine the Manning's friction coefficient in the river and thereby addressing the sub-research question "To what extent can the Manning friction coefficient of the river channel and floodplain for medium to large rivers be accurately quantified?"

At the Chache site, the focus will be primarily on the previously established rating curves, elaborated in subsection 2.2.1. According to Kasteel [2023], BPA's current rating curve tends to overestimate discharges at higher water levels. Thus, the newly formulated data-driven rating curve by Kasteel [2023] will also be employed to assess and possibly substantiate the model outcomes with a physically-based approach. Similar assumptions for friction coefficients in the river channel will be applied here as is done at the Bamboi Bridge site. The findings will be compared against the rating curves presented in subsection 2.2.1. Initially, this comparison will only include the results within the river channel and not in the floodplain, i.e., depths lower than approximately 4.5 meters (equivalent to 238.93 meters in relative bathymetric height). The subsequent step involves comparing the friction coefficient in the floodplain. Once again, the coefficient will be determined using the guidelines by Arcement Jr et al. [1984] and compared with the rating curves. However, caution must be exercised when handling heights above approximately 6.57 meters (equivalent to 241 meters in relative bathymetric height) due to the floodplain water's connection to the bathymetry part derived from the SRTM DEM files, which exhibit lower resolution and accuracy. The intention was, similar as at the Bamboi Bridge site, to match the surface velocities in the floodplain calculated using the Delft3D FM model against the surface velocity results calculated using OpenRiverCam. This is not possible, because the fieldwork is conducted during the dry season, where flow rates are nearly negligible, so surface velocity measurements couldn't be conducted. Moreover, there were strong winds in the opposite direction of the flow, which would have led to negative discharges when using LSPIV, rendering them unsuitable for model validation.

3. Results

3.1. River discharge and surface velocities

3.1.1. Result

Bui Bridge: On March 10, 2023, two UAV videos were captured at the Bui Bridge site, which is located 1.7 kilometers downstream of the Bui Dam. The purpose of these videos was to assess the accuracy of OpenRiverCam in middle to large rivers using the discharge measurements obtained by BPA, which monitors the turbine discharges at the dam. The lag time is determined during the fieldwork. A message was sent when the second turbine was turned on, resulting in a doubling of the discharge. This led to a change in water height in less than 30 minutes. The recorded discharges of the Bui Dam during this day are shown in Appendix Figure C.2, unit 4 (the turbinette) has a constant ecological flow of 14 m³/s which has to be added to the total discharge. The first video was recorded at 10:57 AM, corresponding to a recorded discharge of 163 m³/s at the dam, while the second video was recorded at 01:28 PM, corresponding to a recorded discharge of 315.5 m³/s at the dam. Unfortunately, a third video was not captured on this day when all three turbines were generating electricity because this was not expected to happen. The cross-sections used in the analysis are a combination of the wet-bathymetry results shown in Figure 3.5a.

		Quantile				
Video	Cross-section	0.05	0.25	0.5	0.75	0.95
1	1	178	197	215	239	258
	2	161	199	220	245	260
2	1	259	281	302	338	379
	2	216	248	283	324	381

Table 3.1.: The discharge quantiles of OpenRiverCam results from the recordings at the Bui Bridge site on $10-03-2023$. The outflow measured at the Bui Dam during the first video is 163 m³/. While for the second video, this is 315.5 m³/s.

Table 3.1 and Figure 3.1 show the OpenRiverCam results. The results are compared with the outflow from the turbines of the Bui Dam. The first video overestimates the discharge significantly. The second video underestimates the discharge little. These variations can be attributed to several factors. For example, the river's non-uniform nature, characterized by substantial rocks at its core, generates significant velocity disparities leading to larger errors. Another contributing aspect could be the velocity index, a parameter typically utilized to convert free-surface velocities into depth-averaged velocities. OpenRiverCam implements a standard value of 0.85, commonly applied in studies of natural channels. However, this

default value assumes mean streamwise velocity profiles following the standard logarithmic-law distribution. Nonetheless, various research suggest that the velocity index is (among other factors) dependent on the Reynolds number [Johnson and Cowen, 2017]. The partly turbulent flows within the river, yield a higher Reynolds number, potentially influencing the velocity index. Additionally, there may be a measurement error in the obtained cross-sections. Improvements in the quantile range have primarily been achieved through two key steps. Firstly, by increasing the step size between numerous points within the cross-section using a method that replaces values within a certain window size with the mean of their neighboring values. The second step involves masking values when their deviation exceeds a specified tolerance threshold of 0.7.

| (a) | (b) |
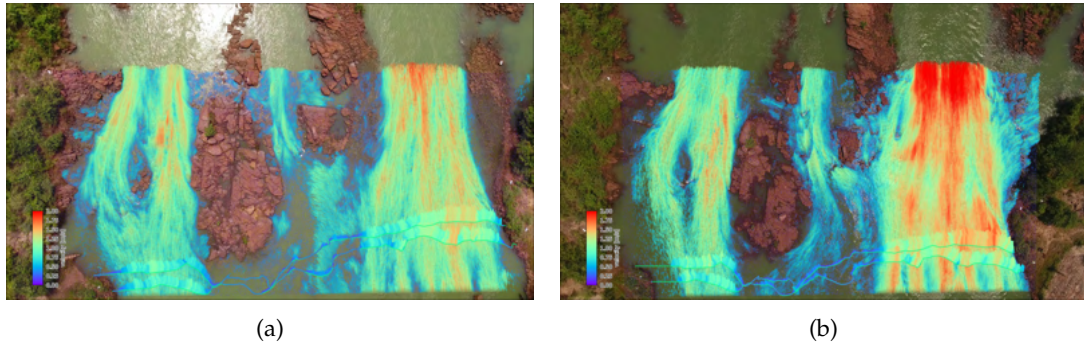
Figure 3.1.: OpenRiverCam results at the Bui Bridge on March 10, 2023: (**a**) A discharge of 217 m³/s at 10:57 (**b**) and a discharge of 304 m³/s at 13:28.

Bamboi Bridge: Five videos were recorded on March 21 and 22, 2023, at the Bamboi Bridge site, situated 32.2 kilometers downstream of the Bui Dam. The travel time of the discharge is approximately 12 hours, and the height differences are less compared to the Bui Bridge site due to mitigated height waves. Also, a significant river tributary between the Bui Dam and the Bamboi Bridge contributes to the overall river discharge. The expected discharges for the recorded videos on March 27 in the morning, afternoon, and March 28 in the morning are hard to determine as will be explained in subsection 3.3.1. Video C.1a captured in the morning displayed favourable tracking conditions with noticeable particle movement and lead to relative good results for cross-sections 1 and 2. However there was a lot of wind influencing this measurement. The third cross-section lacked sufficient eddies or debris for accurate LSPIV tracking, resulting in a big difference in discharge with the other cross-sections. More results can be found in Appendix C.1. It is important to emphasize that, beyond discharges, surface velocities also carry significance for the 3D model, as explained in Section 2.5. These velocities are effectively depicted in Figure 3.2. From fieldwork experience and the surface velocity result, two different values are chosen. The first surface velocity is for the deeper part of the river in the middle and is approximately 1.0 m/s. The second surface velocity in the shallow part at the river sides is approximately 0.15 m/s. However, their accuracy should be approached with prudence.

Chache: The fieldwork is carried out during the dry season, a period when flow rates are almost negligible. As a result, surface velocity measurements could not be performed. Additionally, unfavorable wind conditions would have resulted in negative discharges if LSPIV were employed, making them unsuitable for validating the model.
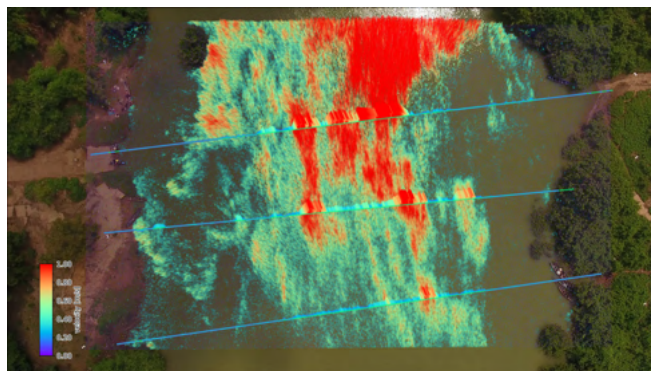
Figure 3.2.: OpenRiverCam result from the first recordings at the Bamboi Bridge site on 21−03−2023

3.1.2. Discussion

The LSPIV technique performed well at the Bui Bridge site, accurately tracking surface velocities by capturing eddies and particle movements in the water. However, the measurement of discharge still lacks accuracy, primarily due to the non-uniformity of the river, but also due to the velocity factor, the post-processing, the smoothing factors and the challenges in measuring the cross-sections. Consequently, comparing the LSPIV results with turbine outflow becomes challenging, and further improvement of post-processing for LSPIV was not extensively pursued.

Challenges were also encountered at the Bamboi Bridge site, including the unknown lag time, attenuating wave heights, limited measurements, and the presence of a different river tributary. These factors made it difficult to compare discharge measurements in the river, and the LSPIV results obtained at this location were also limited in their success. As a result, less focus was given to the further improvement of LSPIV post-processing in these areas.

The Bamboi Bridge and Chache site poses challenges for obtaining accurate results with LSPIV due to various physical factors such as the large width of the river, relatively low surface velocities, wind and sun reflection. These factors introduce uncertainties and affect the precision of the measurements. The processing time and memory required for applying LSPIV videos across the entire river width are substantial, especially when assessing the whole area captured in the recording. In order to achieve better results, it would have been beneficial to capture more videos using the UAV from different angles. This would have provided varying lighting conditions on the river, which might have improved the effective tracking of the particles using LSPIV. Applying LSPIV to a smaller section of the river is with the current version of OpenRiverCam not yet possible, as defining six different GCPs becomes challenging due to the lack of distinctive features on both sides of the focused frame. Therefore, careful consideration is necessary when using OpenRiverCam for data collection and analysis in these types of rivers. However, it should be acknowledged that locations with higher surface velocities, more turbid sections or smaller sections of the river, still offer the potential for effectively utilizing LSPIV in these types of rivers. In addition, there can be anticipated on these challenges when a permanent video measuring station is established.

3.2. Bathymetry

3.2.1. Dry bathymetry

The dry bathymetry is captured using photogrammetry with the Phantom 4 UAV. To ensure the capture of all bathymetric data, a combination of two separate grids is flown. Firstly, a double grid is flown with an 80 percent side- and forward overlap at a height of 90 meters and with an angle of 20 degrees oblique (20 degrees forward from the downward (nadir) view). The 20-degree oblique flight angle serves a dual purpose: it captures a comprehensive view of the terrain even under vegetation cover and mitigates the potential for light reflections on the water surface caused by ripples. Secondly, a circular grid is flown with a flight height of 45 meters, capturing images at 7-degree intervals (resulting in approximately 52 photos). The camera angle for the circular grid is adjusted based on the dimensions of the surveyed area. Every study site has an area of approximately 80.000 square meters considering the limitations imposed by battery life (three batteries). This area is considered sufficient for an accurate representation of the bathymetry. An example of a grid is shown if figure 3.3.

Figure 3.3.: Flight plan, from: Pix4Dcapture [2018].

The obtained two-dimensional images from the study sites are converted into a three-dimensional point cloud using Structure from Motion (SfM) derived photogrammetry software called WEB Open Drone Map (WebODM). This can be done by pre-calibration or by calibrating 'on-the-job' using structure-from-motion and a self-calibrating bundle adjustment. Both calibrations are compared for each study site with 6 to 7 GCPs and the error is the lowest for all the on-the-job calibrations with a maximum RMSE of 0.022 meters. Attention should be paid to these summary error statistics, they may mask vertical systematic errors, such as 'doming' or 'bowling' Griffiths and Burningham [2019]. The GCPs, which have an area of approximately 1.6 square meters and are precisely located using RTK-GNSS, not only facilitate the calibration process but also make it possible to combine the dry -and wet bathymetry using a similar spatial reference system.

The point clouds are processed and interpolated as described in subsection 2.4.1 to ensure the most accurate representation of the dry bathymetry. For addressing the issue of vegetation-induced noise, two filtering methods were employed. The first method involved

(a)   (b)

Figure 3.4.: 3D point cloud of (**a**) the Bui Bridge site (03/03/2023) and (**b**) the Chache site
  (16-03-2023), made with: OpenDroneMap [2023])

masking the specific area affected by vegetation noise and performing a new interpolation on
the entire bathymetry dataset. The second method utilized the Grass GIS tool r.geomorphon
to remove the vegetation-induced noise. After comparing the two filtering approaches, it
was determined that the masking method yielded superior results due to its targeted focus
on the area with vegetation noise. This makes sense because this is done by hand. However,
it is important to note that the r.geomorphon method resulted in almost similar results, is
less time consuming, can still provide satisfactory outcomes and can be applied to larger
areas. The final dry bathymetry is purely based on a geo-spatial approach.

3.2.2. Wet bathymetry

Photogrammetry cannot measure water depths in the river due to the turbidity of the wa-
ter of the Black Volta River. Therefore, the Deeper Sonar Chirp+ was utilized for depth
measurement in combination with RTK-GNSS to achieve a horizontal accuracy of less than
2 centimeters and a vertical accuracy of less than 10 centimeters (based on a 2.1% vertical
accuracy of the maximum depth). The use of the RTK-GNSS is also required for combining
the dry- and wet bathymetry. The results of this approach are presented in Figure 3.5. At
the Bui bridge site, the high velocities posed difficulties for using a canoe to navigate the
measurement grid. Instead, a rope was suspended from the bridge, but this method also
affected the accuracy of the results. In certain locations, the sonar measurements registered
the second or even third reflected signal as the depth, resulting from signal disruptions of
the Deeper Sonar Chirp+. These disruptions were caused by imbalances created by eddies
and swirling in the water, leading to an overestimation of the actual depth by two or three
times. Fortunately, the true values were available in the Fish Deeper application, although
manual conversion was required. Additionally, due to gaps caused by signal loss, only two
reasonable cross-sections could be created from the four back-and-forth passes. In contrast,
the canoe-based bathymetric data proved to be a more accurate and effective solution, and it
was successfully used at both the Chache and Bui Bridge sites. Upon analysis of the Chache
study site results, it was discovered that the depths close to the West side of the grid de-
creased abnormally due to settled sand near the new bridge. As a result, only the unaffected
measurements on the East side were utilized in the subsequent steps.

The curvature of the river cross-section makes direct interpolation between the measured

(a)

(b)

(c)
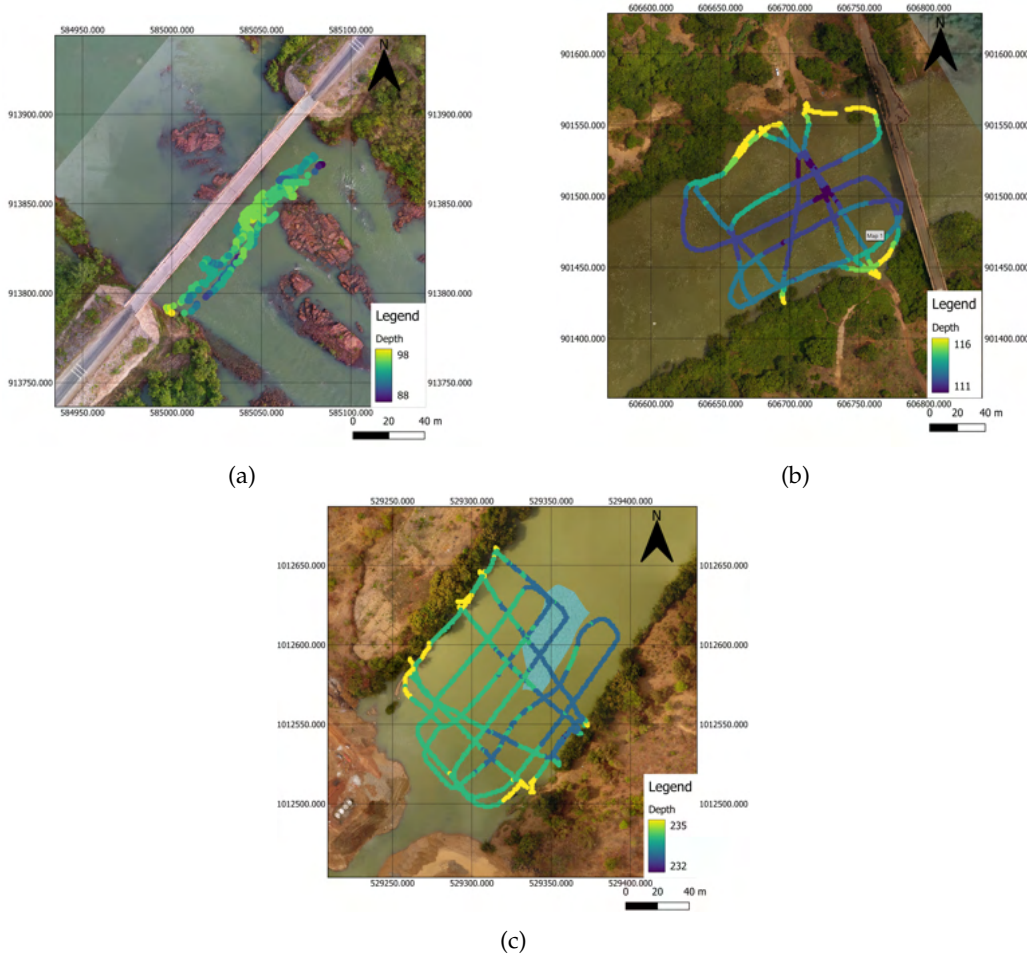
Figure 3.5.: Sonar measurements: (**a**) Bui Bridge, a floater with a rope held from the bridge, (**b**) Bamboi Bridge, a floater sailed with a canoe, (**c**) Chache, a floater sailed with a canoe.

sonar points an inaccurate representation of reality as is explained in subsection 2.4.2. To solve this problem, a higher 'importance' to the orthogonal grid lines is desired when interpolating. To achieve this, the following steps have been applied: (also shown in 3.6 and Appendix A). Firstly, the grid is rotated, to have the river flow direction parallel to the x-axis. Secondly, the grid is scaled in the y direction creating larger distances between the grid lines that are directed parallel to the river flow. Thirdly, the grid is interpolated to obtain the DEM. Due to the scaled distances, the impact of the orthogonal grid lines is far greater than that of the parallel ones. Finally, the DEM is scaled and re-rotated back to its original resolution and orientation, resulting in a DEM that accurately follows the curvature of the river. The DTM of the dry-bathymetry acquired through UAV surveying is larger in scale compared to the DTM of the wet-bathymetry. In order to estimate representative values for the wet-bathymetry in areas where data is missing, a mean cross-section is determined which shifts with the curvature of the river. The slope of the river is added over the direction, parallel to the flow direction. This approach is feasible due to the consistency and homogeneity of the river at the sites. The Bui Bridge bathymetry was not interpolated due

to the limited number of sonar measurements and the heterogeneous nature of the riverbed, which made it challenging to make reasonable assumptions.
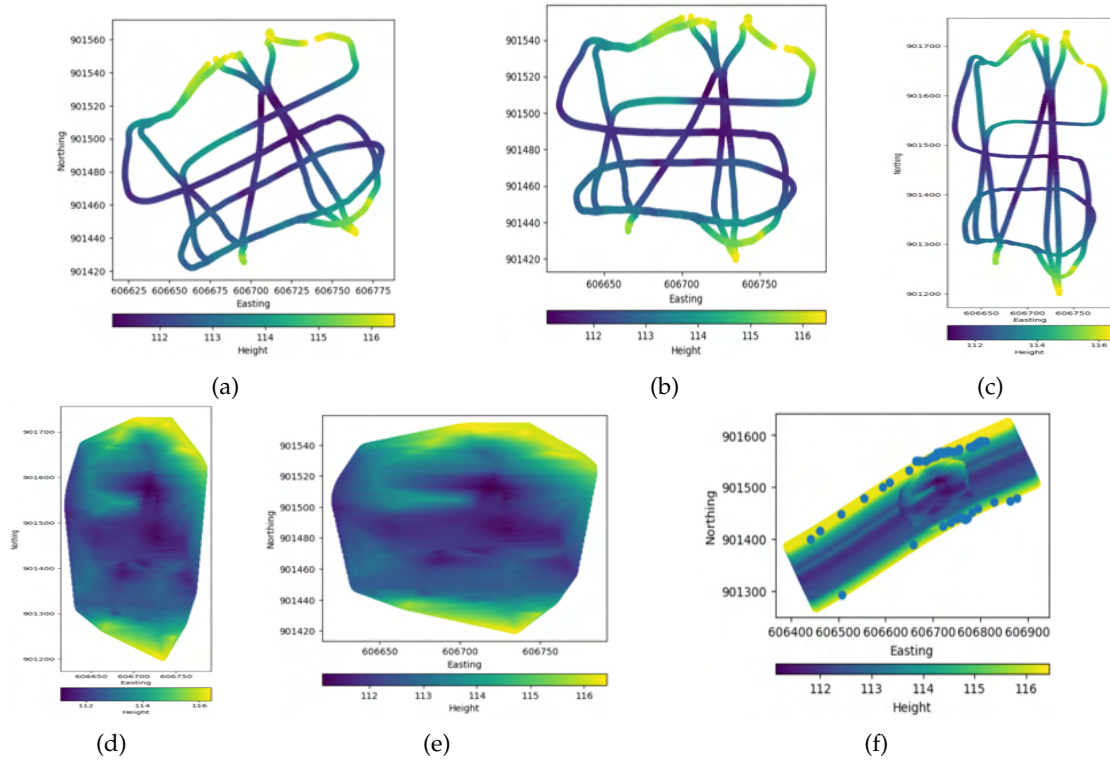
Figure 3.6.: Bamboi Bridge Sonar Measurements: (**a**) Initial measurement. (**b**) Rotated. (**c**) Scaled in y-direction. (**d**) Linear interpolated. (**e**) Re-scaled. (**f**) Re-rotated and the mean values per row shifted parallel to the meandering of the river (the blue dots corresponds with the riversides).

The slope of the river could not be measured directly during the fieldwork, due to obstructing vegetation, hindering a clear signal transmission between the RTK-GNSS rover and base. Instead, the slope was determined using the photogrammetry point cloud data, which indicated a slope of 0.0003. Additionally, several Shuttle Radar Topography Mission (SRTM) Digital Elevation Maps were utilized, resulting in an average slope of 0.0002 over a 30 kilometers stretch of the river. For further calculations, a slope value of 0.0003 was employed. The measurement obtained from the photogrammetry data appears to be representative in this case and is used in further processes.

3.2.3. Combined bathymetry

In order to create the full bathymetry, the wet- and dry bathymetry are merged in two steps. First, the GRASS GIS tool "r.patch.smooth" is utilized to merge and smooth the overlapping bathymetric sections. Second, the gaps in the bathymetry are interpolated linearly using the QGIS fill-gaps tool, the overall obtained resolution is 0.01 square meters. The results are displayed in Figure 3.7.
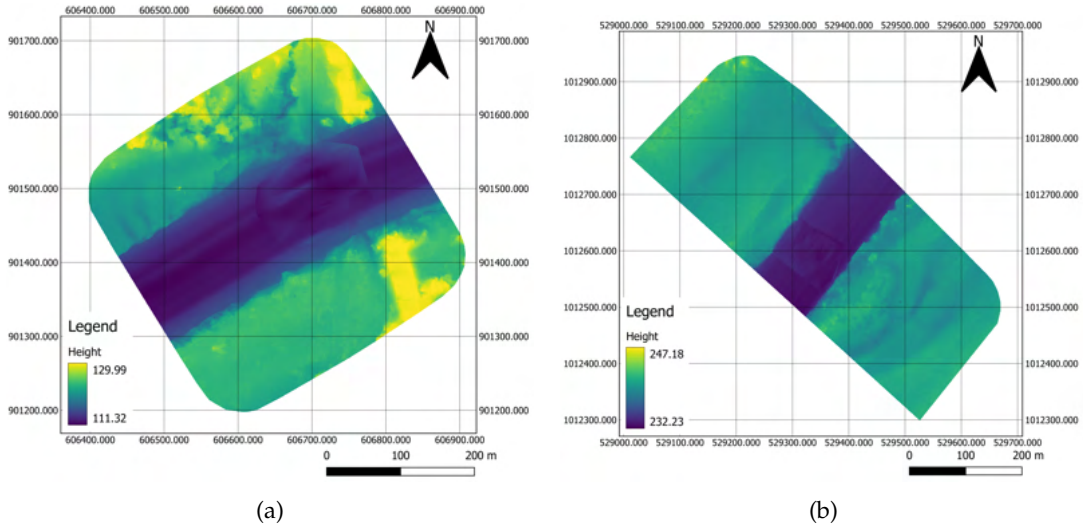
Figure 3.7.: Full bathymetry: (**a**) Bamboi Bridge, (**b**) Chache

The bathymetric data covers a 400x400 meter area at the Bamboi Bridge site and a 250x600 meter area at the Chache site. However, it should be noted that at the Chache site, the floodplains are wider. The UAV Photogrammetry could not capture this entire floodplain due to its limited battery life. To address this, the bathymetric data is extended by integrating SRTM Digital Elevation Maps, which have a tile width of 30x30 meters, see Appendix B.1. While not ideal, this approach matched the existing data reasonably. However, the absolute accuracy of bathymetry outside the 400x400 meter area is considerably lower as a result. This will certainly be taken into account while analyzing the data in the model.

To utilize the merged bathymetric data in the Delft3D FM Suite 2.5, additional steps are taken to ensure a steady state representation of the river throughout the entire bathymetric model. This involves extending the length of the river. The complete bathymetry data is imported into Python once again and the bathymetry is extended based on the full cross-sections both upstream and downstream. This extension ensures that the downstream boundary conditions have a negligible influence on the results. The extended bathymetry data is then converted into an XYZ-file format, which facilitates importing into the Delft3D FM Suite. Once imported, the bathymetry is interpolated matching the grid size of the model, as depicted in Figure 3.8.

3.2.4. Discussion

Photogrammetry using a UAV and WebODM is a highly effective and user-friendly method for determining dry bathymetry, despite the various possible ways in which the photos can be collected. However, it is important to consider the limitations associated with this approach. First, the drone's battery life (even with 3 batteries) sets a constraint on the area that can be covered in a single flight, necessitating careful planning to ensure sufficient coverage. Second, the processing time required in WebODM to convert the captured images into a detailed point cloud can be time-consuming, particularly for large data sets. Lastly, densely vegetated areas at the riverbanks, pose challenges in accurately determining the terrain.

By recognizing these limitations and implementing appropriate mitigation strategies in the flight as explained in 2.4.1, the photogrammetry-based method has successfully delivered high-accuracy and efficient point clouds.

The use of the Sonar Deeper Chirp+ in conjunction with RTK-GNSS has also proven to be an effective method for determining wet bathymetry, provided that the flow velocities in the river are not too high. However, it is important to consider the limitations associated with the RTK-GNSS device connected to the phone. The device may not be robust and can be challenging to waterproof. This is partly due to the requirement of an unobstructed Lo-Ra connection between the rover and the base station, as well as the need to frequently check the results on the phone. Despite these limitations, the combined use of the Sonar Deeper Chirp+ and RTK-GNSS offers a valuable approach for determining wet bathymetry. At the Bui Bridge study site, due to the heterogeneity of the wet bathymetry and the relatively limited acquired sonar data, a full bathymetry couldn't be adequately constructed. The lack of realistic values for areas without sonar measurements led to this limitation. Conversely, the homogeneity of the Black Volta River at the Bamboi Bridge and Chache study sites enabled a reliable bathymetry. In hindsight, it may have been better to survey a larger area, but given the homogeneity of the river, it seems that the results are not much affected. Additionally, interpolating the results using scaling proved to be highly representative of the wet bathymetry. However, the actual accuracy of this method cannot be compared.

During the fieldwork, it was not possible to determine the slope of the river due to the dense vegetation along the riverbanks and the requirement for an unobstructed connection between the base and rover during measurements. Therefore, the slope was estimated as accurately as possible using the photogrammetry point cloud and also using SRTM DEM tiles. However, the actual accuracy of these estimations remains also unknown. Using SRTM DEM tiles to estimate the area in the floodplain with no data is a rough approximation. In subsection 3.3.1, it is evident that these DEM tiles are not accurate enough for calibrating the friction coefficient. Although the use of SRTM files for areas without available data in the floodplain seemed to align well with the areas where data was present, more attention should be given to this step. Despite the bathymetry being less accurate in the floodplain where the SRTM DEM tiles are added, the overall bathymetry now appears to be a good representation of reality.

3.3. 3D Model

3.3.1. Result

Two distinct Delft3D FM models have been developed, corresponding to the Chache and Bamboi Bridge sites. These models incorporate all the gathered and processed data. The initial step involves the incorporation of bathymetric data. The bathymetric length of each model is dependent on the boundary conditions. By setting the lower boundary condition at a greater distance, it effectively isolates the area of interest from the influence of the boundary conditions, allowing for a steady uniform flow conditions and an accurate representation of the system's behaviour within this area of interest. To verify this, the slope of the river is examined. The slope of the riverbed should match the slope of the water depth in the studied area. Figure 3.9 illustrates this alignment for two arbitrarily selected flow values (200 m³/s and 2000 m³/s) at the Chache study site and two arbitrarily selected friction coefficients (0.1 and 0.05 s/m$^{1/3}$) at the Bamboi Bridge site. The Bamboi Bridge site is

modelled with dimensions of 5 kilometers in length and 0.4 kilometers in width. Similarly, the Chache site is modelled with dimensions of 6 kilometers in length and 1.7 kilometers in width. Every grid cell has an equal layer distribution of ten layers, making it a three-dimensional model. For the derivation of a rating curve, various discharges are used as upper boundary conditions. A rating curve can be established when the slope of the river matches the slope of the riverbed and a consistent, uniform flow is achieved. Additionally, depth-averaged velocities are computed, facilitating their comparison with OpenRiverCam surface velocities, as elaborated in Section 2.5.

(a)   (b)
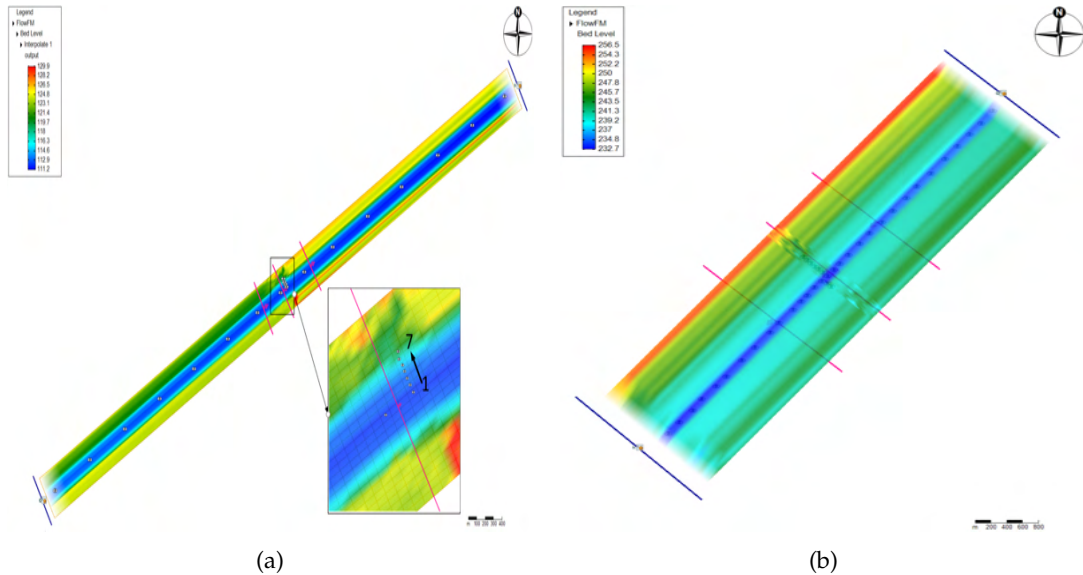
Figure 3.8.: Delft3D FM Suite models showing the river bed: (**a**) Bamboi Bridge 5.8 x 0.4 kilometers, zoomed in on the observation points corresponding to Figure 3.11 going from the middle section to the side of the river. (**b**) Chache 6 x 1.7.

Bamboi Bridge:

Based on Appendix Figure C.3 regarding the Bui Dam outflow, the discharge in the Black Volta River at the Bamboi Bridge is expected to range between 140 and 360 m³/s. The distance between the Bui Dam and the Bamboi Bridge is approximately 32.2 kilometers. Considering the upstream boundary condition located 3 kilometers upstream and assuming a mean velocity of 0.7 m/s, it is expected that the lag time between the Bui Dam and the Bamboi Bridge is 12 hours. However, the accuracy of this mean velocity will be analyzed later. Since the LSPIV technique yielded satisfactory results in the first video it will also be used for comparison. The video was captured at 10:24 on March 21, 2023. Unfortunately, there is no available data for the discharge at 20:24 the previous day, except for the knowledge that two turbines were operating between 18:00 and 24:00. Considering the average discharge on March 21, 2023, it is expected to be around 344 m³/s at that time. However, it could be slightly lower as well, considering that after 24:00, only one turbine (+ turbinette) is in operation (refer to Appendix Figure C.3), leading to a gradual attenuation of the discharge. To gain a comprehensive understanding, Figure 3.10a is created. It shows the water heights (measured with the RTK-GNSS) over time and the measured outflow from the Bui Dam including a 12 hour lag time.

(a)	(b)
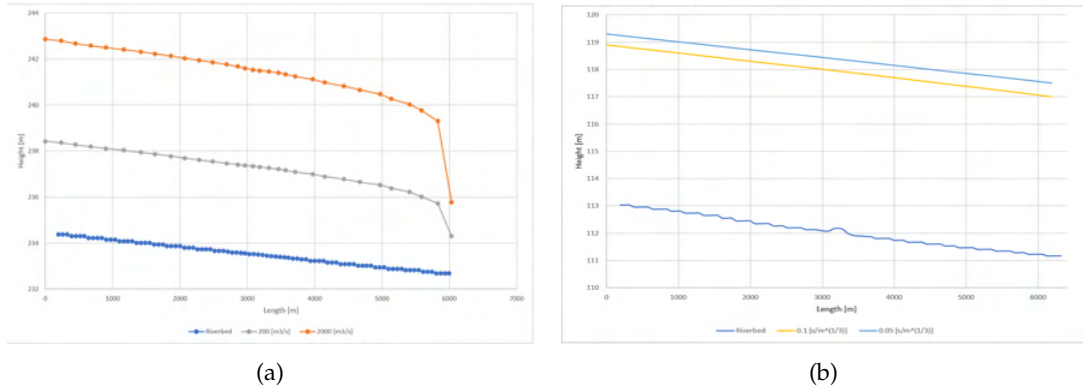
Figure 3.9.: Delft3D FM Suite models showing the slope of the river bed and water height for (**a**) Chache with different discharges and for (**b**) Bamboi Bridge with a different Manning's friction coefficient.

There is no rating-curve established at this site, so the discharges can only be compared to the outflows of the Bui Dam and the OpenRiverCam results. The model is developed, and a rating curve is established between the values of 75 and 450 m³/s with a friction coefficient of 0.05 s/m$^{1/3}$ in the river channel and 0.13 in the floodplain based on assumptions made according to Arcement Jr et al. [1984]. The results are displayed in Figure 3.10b. The measured heights during the fieldwork and their discharges can now be found using this rating-curve and compared with the discharges measured at the Bui Dam, Table 3.2 shows an overview. The assumed average velocity of 0.7 m/s was validated and found to be correct (0.72 m/s for 360 m³/s).

Measurement	Time	Height [m]	Discharge [m³/s]		
			Bui Dam (+12 hours lagtime)	Delft3D FM	OpenRiverCam
1	21/03/2023 10:24	117.103	344	363	170
2	21/03/2023 12:09	116.905	145	339	N.A.
3	21/03/2023 15:05	116.812	145	328	N.A.
4	21/03/2023 15:57	116.732	145	318	N.A.
5	22/03/2023 08:39	117.532	355	433	N.A.

Table 3.2.: The measured and calculated depths and discharges of the Bamboi Bridge site.

The first measured height corresponds to a discharge of 362 m³/s. The measured outflow at the Bui Dam is 344 m³/s, so this aligns well. Measurements 2, 3, and 4 were taken at the beginning of lower outflows (1 turbine + turbinette), at an outflow of about 150 m³/s. It is plausible that the difference in discharge and consequently the difference in water level is attenuated over time, thus these discharges may be higher. However, the difference is quite significant. This would also imply that the discharge from the first measurement should be lower. Measurement 5 was taken at the start of the following day, with rainfall during the night. The discharge determined with the Delft3D FM model overestimates the discharge significantly compared to the Bui Dam discharges, although this could be attributed to the rainfall. Numerous factors play into the measured discharges. For the outflows at the Bui dam these include susceptibility to attenuation, the presence of a river tributary with unknown discharges between the Bui Dam, and the impact of a rain event with unknown effects and others. Regarding the OpenRiverCam result from video 1 with the average values

(a)

(b)
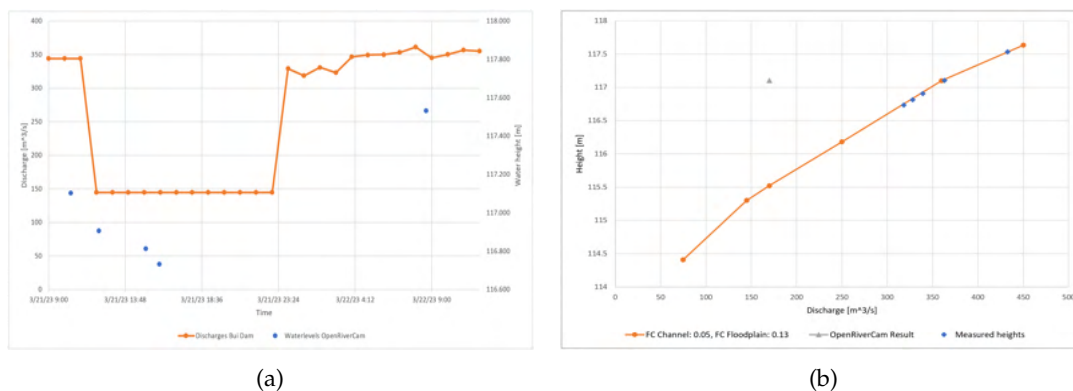
Figure 3.10.: (**a**) The blue line represent the measured water levels at the Bamboi Bridge site. The orange line represents the outflow of the Bui Dam including a lag time of 12 hours due to the distance between both places. This graph facilitates the comparison of the measurement timing with an estimated discharge. (**b**) Rating-curve of the Bamboi Bridge site with a friction coefficient of 0.05 and 0.1 s/m$^{1/3}$ obtained with Delft3D FM Suite. The blue dots correspond with the measured river heights

from the first and second cross-sections of this video (170 m³/s), it appears that the results do not align either. Concerning the Delft3D FM model, an incorrect friction coefficient or slope might exert excessive influence on the outcomes. To summarize, reaching definitive conclusions about the accuracy of either the model or the OpenRiverCam results is quite challenging based on these findings. Hence, to gain a more comprehensive understanding, we compare not only the discharges but also the surface and averaged-depth velocities.

As evident from subsection 3.1.1 is the surface velocity in the middle of the river approximately 1.0 m/s and at the sides approximately 0.15 m/s. By Applying the velocity index of 0.85 [-], this results in depth-averaged velocities of 0.85 m/s in the middle of the river and 0.13 m/s at the sides. The depth-averaged velocities are also calculated with the Delft3D FM model with 3 different discharges at 7 observation points going from the middle section to the side of the river. The results are displayed in Figure 3.11.

Using OpenRiverCam, a discharge of 170 m³/s is calculated. However, the depth-averaged velocities don't match the Delft3D FM findings. Examining the OpenRiverCam surface velocities (Figure 3.2), there are noticeable gaps in the cross-section where no surface velocities were detected. Considering the consistent river flow that is observed during the fieldwork and in the model, it makes sense that the discharge calculated by OpenRiverCam is underestimated. Based on this result, it can be concluded that the model seems to be reasonable. However, due to the factors mentioned earlier, determining accuracy is not feasible, and it remains a challenge to improve the estimation of friction coefficients.

Chache:

At the Chache site, the Delft3D FM model is used to determine different rating-curves and compare them with the rating-curves of BPA and Kasteel [2023]. Also, the averaged-depth velocities are determined for several different discharges, but these cannot be compared with any OpenRiverCam results because of the negligible flow rate during the fieldwork. Assumption are made for the friction coefficient in the river channel and for the floodplain. As at the Bamboi Bridge site, the river channel's friction coefficient at Chache is expected
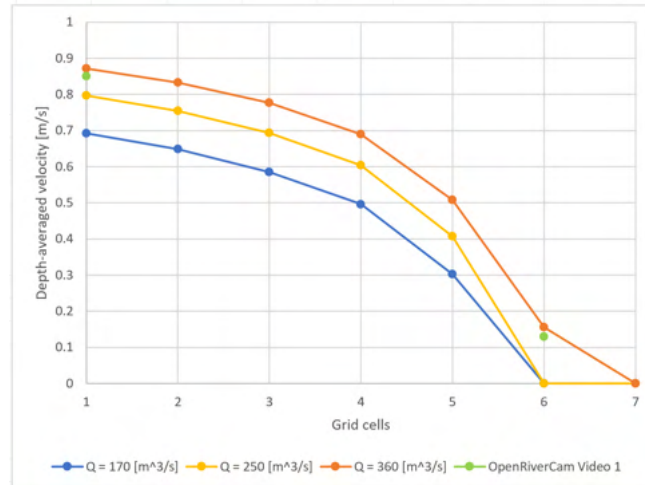
Figure 3.11.: Bamboi Bridge depth-averaged velocity results

to be around 0.04 s/m$^{1/3}$, reflecting characteristics of coarse sand and some vegetation. In the floodplain, the coefficient is projected to vary between 0.11 and 0.14 s/m$^{1/3}$, both in line with Arcement and Schneider's (1984) recommendations

The initial focus is on the river channel, a constant friction coefficient is applied across the entire bathymetry, as shown in Figure 3.12. The analysis revealed that the friction coefficient in the river from the rating-curves are around 0.04 and 0.05 s/m$^{1/3}$, which is consistent with the assumed friction coefficient of 0.04 s/m$^{1/3}$. It's noteworthy that the rating-curve from BPA closely corresponds to a constant friction coefficient across the entire bathymetry. Physically, this might seem inaccurate due to the substantial vegetation in the floodplains, which would logically increase the friction coefficient.
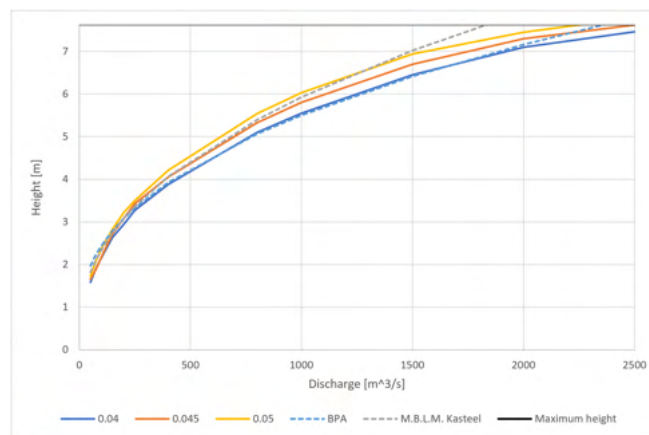
Figure 3.12.: Modelling result of the rating-curve at Chache with constant friction coefficients, 0.040, 0.045 and 0.050 s/m$^{1/3}$ compared with the rating-curve from BPA and Kasteel [2023].

Subsequently, the rating curve is further modelled by varying the friction coefficients. The

friction coefficient in the river is still assumed to be within the range of 0.04 to 0.05 s/m$^{1/3}$, ensuring consistent discharges below 4.5 meters. For the floodplain, friction coefficients of 0.08 and 0.15 s/m$^{1/3}$ were assumed, as illustrated in Figure 3.13. It appears that the best fit with the rating-curve from Kasteel [2023] will align with a friction coefficient of 0.13 s/m$^{1/3}$. Assuming this rating curve offers a more accurate representation than the current BPA rating curve, this highlights the potential of establishing a robust rating curve through a comprehensive approach involving full bathymetry and empirical friction coefficients.

(a)   (b)
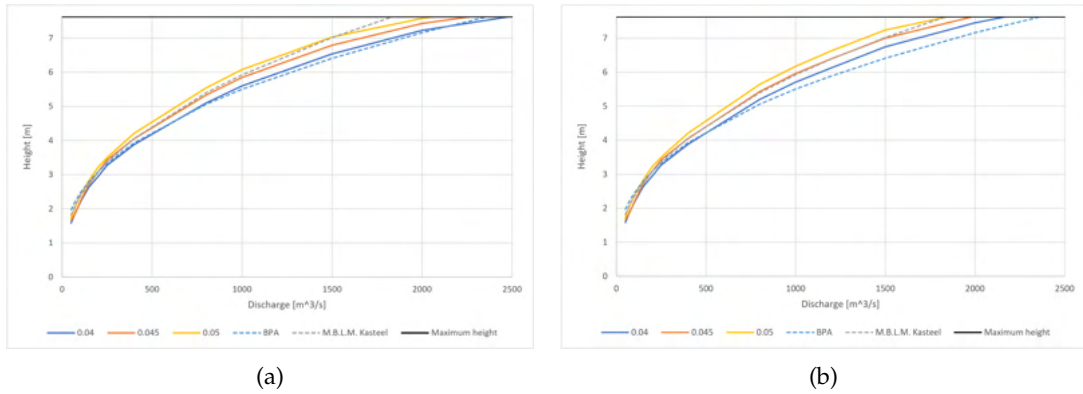
Figure 3.13.: Modelling result of the rating-curve at Chache with friction coefficients of 0.040, 0.045 and 0.050 s/m$^{1/3}$ in the river and a friction coefficient of (**a**) 0.08 s/m$^{1/3}$ and (**b**) 0.15 s/m$^{1/3}$ in the floodplains. The rating-curves from BPA and Kasteel [2023] are added for comparison.

Despite the absence of river velocity measurements (using OpenRiverCam), a graph of depth-averaged velocities has been constructed. This graph is based on a friction coefficient of 0.045 s/m$^{1/3}$ in the river channel and 0.13 s/m$^{1/3}$ in the floodplains. The distribution of observation points follows the same approach as previously done at Bamboi Bridge. These depth-averaged velocities can serve as a valuable resource for potential further research.
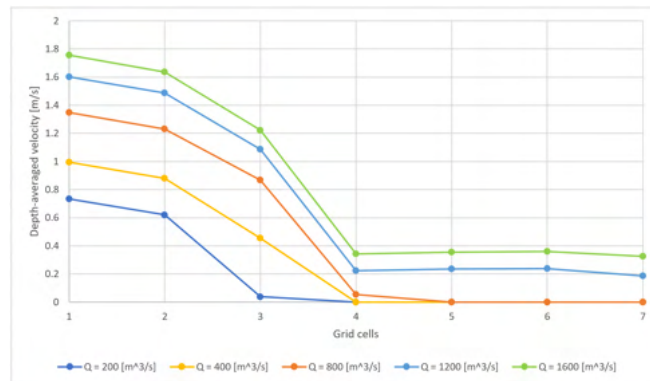
Figure 3.14.: Chache depth-averaged velocity results

3.3.2. Discussion

The successful creation of two three-dimensional river discharge models at the Bamboi Bridge and Chache sites offers valuable insights into the dynamics of the Black Volta River. At the Bamboi Bridge site, the initial intention to directly compare the outflows of the Bui Dam and the Bamboi Bridge was hindered by several factors. The presence of an intervening river tributary, a greater-than-expected distance between the two points, and the introduction of rainfall complicated a direct comparison. Also, it turns out that the discharge results from OpenRiverCam seem to underestimate the actual flow. This conclusion is supported by the model's output, as the significant difference between estimated discharge and measured water levels appears implausible and is also reflected in the examination of depth-averaged velocities from Figure 3.11.

Similarly, the Chache site presented interesting findings regarding the river's behaviour. The original rating curve provided by BPA closely aligned with a constant friction coefficient of 0.04 $s/m^{1/3}$. Physically, this might seem inaccurate due to the substantial vegetation in the floodplains, which would logically increase the friction coefficient. Wen examining the rating curve based on research from Kasteel [2023], the graph started to diverge after a height of 4.5 meters. This divergence can be attributed to the natural characteristics of the river, as water partially flows into the floodplains above this threshold. Both figures deviated significantly above a height of 6.57 meters (equivalent to 241 meters in the relative bathymetric height). This discrepancy is likely due to inaccuracies in the bathymetric data extension when integrating the SRTM Digital Elevation Maps. However, it may also be due to the fact that the floodplain is more heterogeneous and, therefore, more dependent on the location of the measurements. This could lead to the floodplain being wider than average, causing the model to overestimate the discharge for high water levels in certain areas. As a consequence, the friction coefficient in the floodplain is only compared on discharge values between 4.5 and 6.57 meters. The rating-curve of Kasteel [2023] corresponds best with a friction coefficient of 0.045 $s/m^{1/3}$ in the river and a friction coefficient of in the range of 0.08 to 0.15 $s/m^{1/3}$ (with the most overlap of 0.13 $s/m^{1/3}$). When comparing the friction coefficient, a slope of 0.0003 [-] was assumed. It's worth noting that the slope and friction coefficient exert mutual influence. However, conducting a sensitivity analysis of the slope uncertainty is complex, primarily due to the necessity of conferring this slope solely to the wet bathymetry. This implies a sequential process of merging with the dry bathymetry, interposed with intermediate steps, followed by an extension to account for boundary condition impacts (as outlined in section 2.4), making it a demanding task. The river discharge models provide significant insights into the hydrodynamics of the Black Volta River, highlighting the potential for establishing a robust rating-curve using empirical friction values and comprehensive bathymetric data. Integrating OpenRiverCam (when the discharge is not negligible) can further enhance accuracy by aiding a more precise selection of the friction coefficients using both the discharge and surface/depth-averaged velocity results.

4. Conclusions

This research has explored various methods and approaches for creating a three-dimensional discharge model and rating curve of a medium to large river using high-precision bathymetry and discharge/velocimetry data obtained from photogrammetry, sonar measurements, RTK-GNSS, and LSPIV.

The data collection methods and assumptions were discussed in detail, efforts were made to obtain this data in an efficient, cost-effective manner with minimal intensive manpower, ensuring a non-intrusive approach. The dry bathymetry was effectively determined using photogrammetry obtained with the DJI Phantom 4 and WebODM. The wet bathymetry was measured by combining depth measurements obtained with the Sonar Deeper Chirp+ and location measurements using the RTK-GNSS. However, obtaining accurate sonar measurements at high water velocities posed a challenge and in order to make data collection easier, it is key to improve the robustness of the measurement equipment. The sub-question, *How can the photogrammetry and sonar measurements be combined to obtain the bathymetry of the river?* was answered in part by effectively merging the photogrammetry and sonar measurements using the same reference points measured with RTK-GNSS. Also, the wet and dry bathymetry underwent individual post-processing through filtering and various interpolation techniques. The biggest challenge to improve this process is the difference in the spatial distribution of the data, making direct interpolation unfeasible. Also, determining the terrain in riverbanks was challenging due to dense vegetation. This same vegetation made it very difficult to determine the slope. Eventually, both bathymetries were smoothly merged and interpolated ensuring a realistic full bathymetry.

To incorporate surface velocities and discharge into the three-dimensional model, the LSPIV technique was utilized with OpenRiverCam, which can convert (UAV) camera videos into surface/river flow velocities using LSPIV. This facilitated the integration of surface velocity and discharge measurements with the bathymetric data. By incorporating these measurements into the model, the sub-question *What are the methods and approaches for integrating surface velocities into a discharge model?* was addressed, leading to a more comprehensive understanding of the dynamics in the river. Different results were obtained using LSPIV depending on the river characteristics. Physical factors such as the large width of the river, the relatively low surface velocities (especially in the dry season), the wind and the sun reflection made it difficult to use LSPIV. However, anticipating these factors when setting up a permanent station could help overcome these challenges. The limited availability of flow velocity and discharge measurements posed a challenge, restricting the comparison to the Chache site and excluding their use in the models.

The three-dimensional models developed in Delft3D FM Suite were subjected to comparison using various approaches. Specifically, at the Bamboi Bridge site, the model was evaluated by comparing it to the discharge results obtained from OpenRiverCam, concurrent water level measurements and outflow measurements at the Bui Dam. Although, the discharge comparison did not yield satisfactory results, it was still possible to compare the surface/depth-averaged velocities suggesting that the accuracy of the model could still be

viable. However, to enhance its accuracy comprehensive data and observations should be gathered. This is particularly crucial in terms of discharge measurements, given the considerable variability in their absolute accuracy.

For the Chache site, two rating curves were compared, considering the physical characteristics of the river. The current rating-curve from BPA closely align the model results when a constant Manning's friction coefficient of 0.04 s/m$^{1/3}$ is assumed in both the river and floodplain. This seems unlikely due to the presence of vegetation on the riverbanks, which should increase the friction coefficient. The rating-curve of Kasteel [2023] corresponds best with a friction coefficient of 0.045 s/m$^{1/3}$ in the river and a friction coefficient of in the range of 0.08 to 0.15 s/m$^{1/3}$ (with the most overlap of 0.13 s/m$^{1/3}$). However, it is recommended to determine the appropriate friction coefficient through velocity and discharge measurements during the wet period to evaluate the reliability and performance of the model. Preferably, during several measurements covering both low and high flows. Without these measurements, it becomes challenging to objectively address the sub-question *To what extent can the Manning's friction coefficient of the river channel and floodplain for medium to large rivers be accurately quantified?* Nonetheless, the results show promising potential.

In summary, this research has successfully tackled the challenges of combining photogrammetry and sonar measurements for accurate bathymetry determination, integrating surface velocities using LSPIV and OpenRiverCam, and quantifying the friction coefficient for medium to large rivers and their floodplains. and thus answered the main research question, ***"How to create a three-dimensional discharge model and rating curve of a middle to large river using a high precision bathymetry based on photogrammetry, sonar, RTK-GNSS and large scale image velocimetry data?"***. The findings contribute to comprehensive understanding of the hydraulic behavior of the river, contributing to improved water flow predictions and management strategies.

5. Recommendations

5.1. Data Collection

Measuring the slope of medium to large rivers with small gradients is challenging, primarily due to the presence of dense vegetation along the riverbanks and the relatively small slope magnitudes. The utilization of RTK-GNSS for slope measurement was impeded by the requirement of an unobstructed line of sight between the base and rover for successful LoRa transmission. An alternative way could be a third sending/receiving LoRA on the water or another type of data transmission between the base and rover. Increasing the distance between measurement points improves accuracy, but again the LoRa connection may present difficulties in achieving these longer distances. In cases where determining the slope proves unfeasible, it is advisable to incorporate the slope uncertainty into subsequent 3D model computations.

The Deeper Sonar Chirp+ had the disadvantage that at high water velocities, the ball would lose balance and partially submerge, resulting in a loss of Wi-Fi signal with the phone and possibly causing the ball to transmit signals at an angle, leading to an overestimation of depths. The Deeper Extender Kit is recommended to prevent this issue Deeper Sonar [nd]. However, it's important to note that the Extender Kit is not tested in this research. Additionally, a good option is to collect the data with the Deeper Sonar Chirp+ attached to a remote-controlled boat. In this scenario, it is important to ensure that the RTK-GNSS system is waterproof and fits on the boat.

To ensure the successful setup of a permanent monitoring station at Chache using LSPIV and OpenRiverCam, it is recommended to conduct initial equipment testing at a nearby location like the Bamboi Bridge site. This step is crucial to minimize the risk of abandonment and ensure a seamless operation of the monitoring system. As mentioned in section 2.2, Chache is a very remote area, making it crucial to function smoothly. Minor mistakes in the installation or software should be avoided. The Bamboi Bridge site is a suitable alternative for testing, as it is only a 30-minute drive away from the local BPA office and shares similar natural river characteristics, especially during the dry season, providing an excellent opportunity to assess its performance and determine if better results with LSPIV can be achieved compared to those obtained in this study. Additionally, the bathymetry data obtained from this research can be utilized, eliminating the need for re-measuring the cross-section. This saves time and effort in the setup process. The Bui Bridge site is also a possibility (even closer), but the natural characteristics of the river are not comparable at this location. It is also advisable to transmit the complete videos captured by the monitoring station, at least during the initial year if feasible. This would allow for an examination of the post-processing procedures employed by OpenRiverCam, thereby enhancing the potential for accuracy improvement. A final recommendation for a permanent setup is to add a wind gauge, to compensate for wind drag to water surface velocity.

5.2. Data Processing

Excessive time and effort were dedicated to the meticulous examination of minor details within the photogrammetry point cloud. Considering the relatively large scale of the numerical model in comparison, it is not essential to allocate such an extensive amount of time to this specific aspect.

It is recommended to conduct a validation experiment on the sonar measurement interpolation by excluding a portion of the data points and comparing the results with a straightforward geospatial interpolation method (one without rotation or scaling). This approach could offer insights into the model's performance and accuracy. Nevertheless, it should be noted that measurement values have not been smoothed, and the measurements are relatively close to each other. So, the differences between methods will be minimal.

After performing scaled interpolation on the sonar measurements, a mean cross-section is determined, which is then used to fill in areas where no data was collected. This approach preserves the actual measured values within the model. It would have been less time-consuming to use the mean cross-section for the entire river because the measured values in the complete bathymetry had a negligible influence. This can be attributed to the larger raster size of the Delft3D FM model, which interpolates the bathymetry across these raster cells. However, the high accuracy of the bathymetry is still required and crucial for accurate results using LSPIV with OpenRiverCam.

One unexplored possibility in this research, with promising potential, is the utilization of photogrammetry to determine the friction coefficient in floodplains. This approach would involve establishing a relationship between the number of points classified as ground and as vegetation in the photogrammetry point cloud and the corresponding friction coefficient. Calibration is crucial to ensure the accuracy and reliability of this method. It would entail comparing the friction coefficients derived from photogrammetry with known values obtained from traditional methods or empirical equations in river systems where such data is available.

The gridding process is mainly centered around a purely geospatial approach, excluding any incorporation of physically based modeling. Therefore, it is recommended that future research explore the utilization of physics-based techniques to enhance bathymetry modelling methodologies.

5.3. Data Modelling

While the model yields realistic values in comparison to the rating-curves established by BPA and Kasteel [2023], it is essential to gather measurements during the wet period to enable a comparison of the discharge and flow velocities and to determine the actual accuracy of the model.

This research has attempted to assess the accuracy of various methods such as OpenRiver-Cam and river discharge modelling using the Delft3D FM models. However, it has proven very challenging due to the limited duration of measurements spanning only one day. This constraint makes it difficult to isolate variables that may impact the accuracy. Therefore, it is advisable to extend the measurement period to gain a more thorough understanding.

Bibliography

Akpoti, K., Antwi, E. O., and Kabo-bah, A. T. (2016). Impacts of rainfall variability, land use and land cover change on stream flow of the black volta basin, west africa. *Hydrology*, 3(3):26.

Arcement Jr, G. J., Schneider, V. R., et al. (1984). Guide for selecting manning's roughness coefficients for natural channels and flood plains. Technical report, United States. Federal Highway Administration. Office of Implementation.

Ardhuin, F., Brandt, P., Gaultier, L., Donlon, C., Battaglia, A., Boy, F., Casal, T., Chapron, B., Collard, F., Cravatte, S., et al. (2019). Skim, a candidate satellite mission exploring global ocean currents and waves. *Frontiers in Marine Science*, 6:209.

ArduSimple (2023). simplertk2b - starter kit lr.

Bandini, F., Olesen, D., Jakobsen, J., Kittel, C. M. M., Wang, S., Garcia, M., and Bauer-Gottwein, P. (2018). Bathymetry observations of inland water¡? xmltex\break?¿ bodies using a tethered single-beam sonar controlled by¡? xmltex\break?¿ an unmanned aerial vehicle. *Hydrology and Earth System Sciences*, 22(8):4165–4181.

Beck, H. E., Zimmermann, N. E., McVicar, T. R., Vergopolan, N., Berg, A., and Wood, E. F. (2018). Present and future köppen-geiger climate classification maps at 1-km resolution. *Scientific data*, 5(1):1–12.

Bertule, M., Glennie, P., Koefoed Bjørnsen, P., James Lloyd, G., Kjellen, M., Dalton, J., Rieu-Clarke, A., Romano, O., Tropp, H., Newton, J., et al. (2018). Monitoring water resources governance progress globally: Experiences from monitoring sdg indicator 6.5. 1 on integrated water resources management implementation. *Water*, 10(12):1744.

BPA (2012). Bui hydroelectric project. *Accra: Bui Power Authority*.

Chow, V. (1959). T. 1959 open-channel hydraulics. *MCGraw Hiu*.

Connor, R. (2015). *The United Nations world water development report 2015: water for a sustainable world*, volume 1. UNESCO publishing.

Deeper Sonar (n.d.). Extender kit.

Deltares, D. (2013). Delft3d-flow user manual. *Deltares Delft, The Netherlands*, 330.

Dinku, T. (2019). Challenges with availability and quality of climate data in africa. In *Extreme hydrology and climate variability*, pages 71–80. Elsevier.

Everard, N., Dixon, H., Sarkar, S., Randall, M., and Schumann, G. (2023). The fluvisat project: Measuring streamflow from space with very high resolution planet satellite video. Technical report, Copernicus Meetings.

Feng, Y., Wang, J., et al. (2008). Gps rtk performance characteristics and analysis. *Positioning*, 1(13).

Fujita, I., Notoya, Y., Tani, K., and Tateguchi, S. (2019). Efficient and accurate estimation of water surface velocity in stiv. *Environmental Fluid Mechanics*, 19:1363–1378.

Griffiths, D. and Burningham, H. (2019). Comparison of pre-and self-calibrated camera calibration models for uas-derived nadir imagery for a sfm application. *Progress in physical geography: earth and environment*, 43(2):215–235.

Johnson, E. and Cowen, E. (2017). Remote determination of the velocity index and mean streamwise velocity profiles. *Water Resources Research*, 53(9):7521–7535.

Jung, H. C., Hamski, J., Durand, M., Alsdorf, D., Hossain, F., Lee, H., Hossain, A. A., Hasan, K., Khan, A. S., and Hoque, A. Z. (2010). Characterization of complex fluvial systems using remote sensing of spatial and temporal water level variations in the amazon, congo, and brahmaputra rivers. *Earth Surface Processes and Landforms: The Journal of the British Geomorphological Research Group*, 35(3):294–304.

Kasteel, M. (2023). Discharge simulation in a data-scarce basin: A case study of the black volta basin.

Kittel, C. M., Nielsen, K., Tøttrup, C., and Bauer-Gottwein, P. (2018). Informing a hydrological model of the ogooué with multi-mission remote sensing data. *Hydrology and Earth System Sciences*, 22(2):1453–1472.

Lehner, B. and Grill, G. (2013). Global river hydrography and network routing: baseline data and new approaches to study the world's large river systems. *Hydrological Processes*, 27(15):2171–2186.

Morrow, R., Fu, L.-L., Ardhuin, F., Benkiran, M., Chapron, B., Cosme, E., d'Ovidio, F., Farrar, J. T., Gille, S. T., Lapeyre, G., et al. (2019). Global observations of fine-scale ocean surface topography with the surface water and ocean topography (swot) mission. *Frontiers in Marine Science*, 6:232.

Mukul, M., Srivastava, V., Jade, S., and Mukul, M. (2017). Uncertainties in the shuttle radar topography mission (srtm) heights: Insights from the indian himalaya and peninsula. *Scientific reports*, 7(1):1–10.

OpenDroneMap (2023). Awesome. drone. software.

Papa, F., Crétaux, J.-F., Grippa, M., Robert, E., Trigg, M., Tshimanga, R. M., Kitambo, B., Paris, A., Carr, A., Fleischmann, A. S., et al. (2022). Water resources in africa under global change: monitoring surface waters from space. *Surveys in Geophysics*, pages 1–51.

Peppa, M., Hall, J., Goodyear, J., and Mills, J. (2019). Photogrammetric assessment and comparison of dji phantom 4 pro and phantom 4 rtk small unmanned aircraft systems. *ISPRS Geospatial Week 2019*.

Pix4Dcapture, S. (2018). Pix4dcapture.

Schumann, G., Matgen, P., Cutler, M., Black, A., Hoffmann, L., and Pfister, L. (2008). Comparison of remotely sensed water stages from lidar, topographic contours and srtm. *ISPRS journal of photogrammetry and remote sensing*, 63(3):283–296.

Bibliography

Shaibu, S., Odai, S. N., Adjei, K. A., Osei, E. M., and Annor, F. O. (2012). Simulation of runoff for the black volta basin using satellite observation data. *International journal of river basin management*, 10(3):245–254.

Stisen, S., Jensen, K. H., Sandholt, I., and Grimes, D. I. (2008). A remote sensing driven distributed hydrological model of the senegal river basin. *Journal of Hydrology*, 354(1-4):131–148.

Van Zyl, J. J. (2001). The shuttle radar topography mission (srtm): a breakthrough in remote sensing of topography. *Acta astronautica*, 48(5-12):559–565.

Westerberg, I., Mansanarez, V., Lyon, S., and Lam, N. (2023). Rapid streamflow monitoring with drones. Technical report, Copernicus Meetings.

Worlddatainfo (2023). Climate comparison: Brong-ahafo / north-ghana.

A. Sonar Interpolation
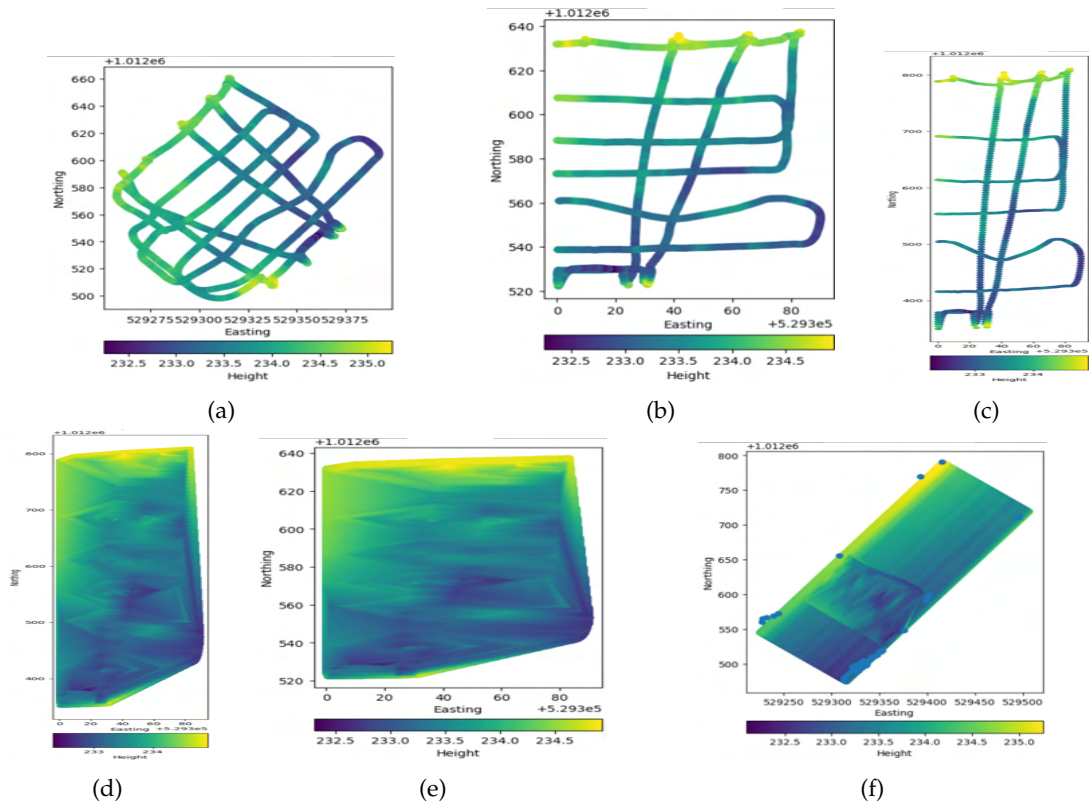
Figure A.1.: Chache Sonar Measurements: (**a**) Initial measurement. (**b**) Rotated. (**c**) Scaled in y-direction. (**d**) Linear interpolated. (**e**) Re-scaled. (**f**) Re-rotated and the mean values per row added (the blue dots corresponds with the riversides).

B. Bathymetry
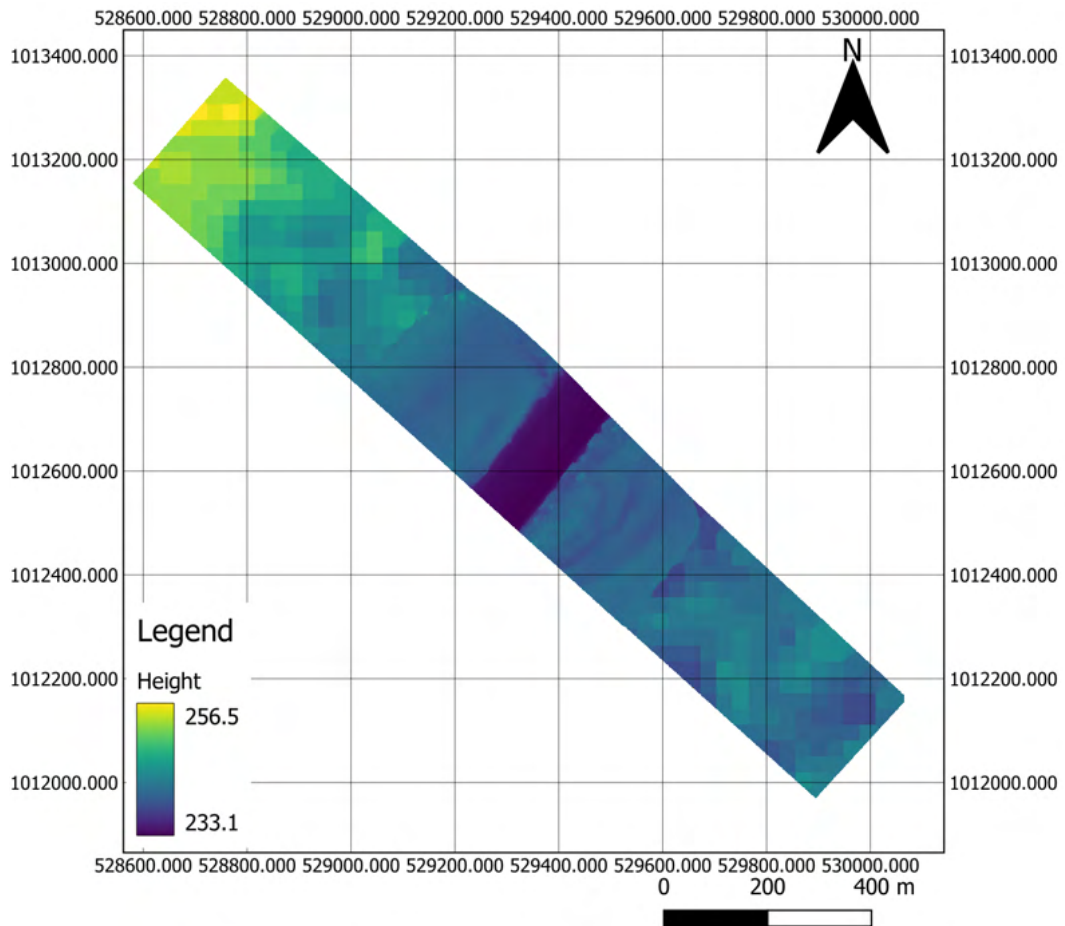
Figure B.1.: Full Bathymetry of the Chache site with SRTM extension from Van Zyl [2001].

C. Discharge measurements

(a)

(b)

(c)

(d)

(e)

Video	Cross-Section 1	0.05	0.25	0.5	0.75	0.95
				quantiles		
1	1	-111.6253	71.39123	177.4791	287.5804	504.6149
	2	-109.8214	53.77513	161.5899	282.6914	491.0015
	3	-191.1566	6.329962	83.76516	191.7368	405.8335
2	1	N/A	N/A	N/A	N/A	N/A
	2	N/A	N/A	N/A	N/A	N/A
	3	-768.3874	-145.989	53.98678	226.6462	707.9126
3	1	-898.4297	-421.05	-122.491	157.3661	625.6691
	2	-942.1283	-445.817	-116.735	185.8096	675.2691
	3	-845.1825	-379.416	-97.0942	174.01165	626.0547
4	1	-75.53098	-23.1088	8.931406	41.56739	98.60718
	2	N/A	N/A	N/A	N/A	N/A
	3	-37.84857	43.57221	93.16966	150.0534	251.2787
5	1	N/A	N/A	N/A	N/A	N/A
	2	-134.4537	-46.5021	-1.537	42.42341	118.3211
	3	-128.2926	-43.4102	0.872796	45.90037	-120.673

(f)

Figure C.1.: OpenRiverCam results: Bamboi Bridge: Video (**a**) at 10:24, 21−03−2023. Video (**b**) Video 2 at 12:09, 21−03−2023. Video (**c**) Video 3 at 15:05, 21−03−2023. Video (**d**) Video 4 at 15:27, 21−03−2023. Video (**e**) Video 5 at 08:39, 22−03−2023. Table (**f**) displays the discharge results.

Video C.1b was taken in the morning, with a lot of reflection due to the sunlight, affecting the results too much. Video C.1c has negative discharge results, which makes no sense. Video C.1d was taken in the afternoon, when the wind had stopped blowing, resulting in

very few particles to track and therefore underestimating the discharge. Video C.1e had almost no particles to track and thus no discharge could be determined. Video C.1f displays the OpenRiverCam discharge results.

BUI POWER AUTHORITY

BUI GENERATING STATION
UNIT READING DISCHARGE SHEET

Day... Friday ....   Date... 10 - 03 - 2023

TIME	UNIT 1		UNIT 2		UNIT 3		UNIT 4
	RATE(m³/s)	VOLUME(m³)	RATE(m³/s)	VOLUME(m³)	RATE(m³/s)	VOLUME(m³)	RATE(m³/s)
01:00					150.2	2564272.8	
02:00					151.1	2958525.4	
03:00					151.3	3303802.6	
04:00					152.2	3766217.9	
05:00					151.1	4266430.5	
06:00					153.1	4666566.4	
07:00					151.4	5099130.9	
08:00					149.4	5599266.2	
09:00					151.3	5994729.1	
10:00					148.8	6406255.1	
11:00					150.1	6773779.3	
12:00					151.2	7231014.9	
13:00	150.2	6321780.7			151.3	7646218.3	
14:00	151.2	6863233.7			150.2	8146539.9	
15:00	153.5	7464695.4			149.7	8746561.2	
16:00	150.4	7994321.2	150.6	25023274	152.1	9246684.8	
17:00	150.2	8478446.4	135.8	2824018.1	151.0	9606560.4	
18:00	151.3	9040552.5	137.0	3373424.4	150.3	0032425.0	
19:00	152.4	9538915.3	137.6	3882310.2	150.4	0432550.6	
20:00	150.1	00603782	158.2	4417677.0	151.3	0932427.2	
21:00	151.4	06397342	169.9	4897844.5	148.9	1287326.7	
22:00	151.6	1240318.4	163.2	5587448.8	150.4	1874789.7	
23:00	160.1	1740977.3	164.6	6173052.5	150.3	2352914.2	
24:00	151.4	2240850.7	144.4	6701549.4	149.5	2752968.5	

TIME	NAME
22:00-07:00	....
07:00-14:00	....
14:00-22:00	....

Figure C.2.: Bui Dam Discharge Measurements on 10-03-2023, Unit 4 has a constant ecological flow of 14 m^3/s (not written down).

BUI POWER AUTHORITY

BUI GENERATING STATION
UNIT READING DISCHARGE SHEET

Day... Tuesday ......

Date... 21 / 03 / 23

TIME	UNIT 1		UNIT 2		UNIT 3		UNIT 4
	RATE(m³/s)	VOLUME(m³)	RATE(m³/s)	VOLUME(m³)	RATE(m³/s)	VOLUME(m³)	RATE(m³/s)
01:00							
02:00							
03:00							
04:00							
05:00							
06:00							
07:00							
08:00							
09:00							
10:00							
11:00			130.5	0678281.8			
12:00	174.2	0079498.7	140.7	1205684.2			
13:00	179.2	0726533.2	131.5	1689674.8			
14:00	179.2	1337364.4	37.6	2046500.8			
15:00	175.2	2184879.2	133.6	2831604.3			
16:00	175.7	2784151.9	157.0	3368393.2			
17:00	175.2	1337364.4	160.2	3710D984			
18:00	175.7	4036038.8	160.2	4479613.9			
19:00	175.7	45015560	167.3	4887000.2			
20:00	182.6	5150905.6	164.8	5469900.8			
21:00	175.7	5743413.7	155.2	600796/.1			
22:00	175.7	6547957.2	160.5	6515772.8			
23:00	179.2	7004408.4	168.3	7157545.3			
24:00	179.2	7780861.5	162.2	7864306.0			

TIME	NAME
22:00-07:00	Fatahu, D. Ofori, Kwakye & Nyami
07:00-14:00	Okene, Adda & Carl
14:00-22:00	Barnes, Ofori, Dominic, Dansa & Carl

Figure C.3.: Bui Dam Discharge Measurements on 21-03-2023. Unit two has an approximate discharge of 130 m^3/s from 01:00 to 10:00 (not written down). Unit three is not turned on this day. Unit 4 has a constant ecological flow of 14 m^3/s (also not written down).

D. Areal photos of the study sites

Figure D.1.: Areal photo of the Chache site, taken on 16-03-2023.

Figure D.2.: Areal photo of the Bui Bridge site, taken on 03-03-2023.

Figure D.3.: Areal photo of the Bamboi Bridge site, taken on 21-03-2023.